Development of SMPD3 deficient pre-osteocytic cell culture models

by

Aishwaria Scaria, MSc

Faculty of medicine

Division of Experimental Medicine

McGill University

Montreal, Quebec, Canada

October 2022

A thesis submitted to Mcgill University in partial fulfillment of the requirements for the degree of Master of Science

Dedication

I dedicate this thesis to my best friend-Jesus, parents: Papa- Mr. Scaria Thomas, Mumma- Mrs. Sincy Scaria, siblings: sister-Amarthya Scaria, brother- George Scaria and enthusiastic inspirer-Meet Erda.

Table of Contents

Acknowledgements-*5*
Contribution of Authors-*7*
Abbreviations-*8*
Abstract-*9*
Résumé-*11*
Chapter 1: Introduction (Context) and Literature Review-*13*
1. Biomineralization-*15*
1.1. Evolutionary importance-*15*
1.2. Comparison between invertebrate and vertebrate mineralization- *16*
1.2.1. Ectopic calcification – *17*
1.2.2. Vertebrate mineralization- *18*
1.3. Mineralized tissues in vertebrates- *19*
1.3.1. Mineralized dental tissues- *19*
1.3.2. Mineralized skeletal tissues- *22*
1.4 Bone as a mineralized tissue: Cell types and development- *24*
1.5 Determinants of physiologic mineralization- *28*
1.5.1. Systemic levels of calcium and phosphate ions- *28*
1.5.2. Collagen scaffold- *29*
1.5.3. Inhibitors- *30*
1.5.4. Intracellular enzymes- *33*
1.6. Revisiting the matrix vesicle theory- *35*
1.7. In vitro cell culture models to depict bone mineralization- *37*
1.7.1. Secondary cell lines- *37*
1.8. Extracellular matrix proteins and mineral deposition- *38*
1.9. CRISPR/Cas9 as a tool for DNA modification- *41*
1.10. Figures
Figure 1- *45*
Figure 2- *46*
Figure 3- *47*
Chapter 2: Objectives- *48*
Chapter 3: Material and methods-*51*
3.1. Treatment of MLO-A5 Cell Line with GW4869- *52*
3.2. Calcein-DAPI staining for in-vitro mineralized cell culture- *52*
3.3. Designing guide RNA (gRNA) oligonucleotide for CRISPR construct- *53*
3.4. Cloning and Transformation- *53*
3.5. Generation of Smpd3 knockout plasmid- *54*
3.6. Transfection- *54*
3.7. Puromycin selection- *54*
3.8. Single cell clone culture- *55*
3.9. Genomic DNA isolation from single-cell clones generated using Smpd3 knockout construct- *55*
3.10. Q5 PCR to target altered sequence- *56*

3.11. Sub-cloning of single cell clone fragments- *56*
3.12. Transformation for subcloning- *56*
3.13. DNA purification and sequencing- *57*
3.14. Gene Expression analysis for Smpd3 KO MLO-A5 clone- *57*
3.15. Mineral deposition analysis- *57*
3.16. Scanning electron microscopy (SEM) and energy-dispersive X-ray spectroscopy (EDS) characterization of MLO-A5 cells- *58*
Chapter 4: Results- *59*
4. 1. Developed SMPD3 inhibitor MLO-A5 model using pharmacological agent-GW4869- *60*
4.2. Generation of SMPD3 knockout model using CRISPR-CAS-9 vector- *60*
4.3. Generation and screening of a Smpd3 knockout model using CRISPR approach- *61*
4.4. Development and detection strategy for clones with homozygotic mutations- *62*
4.5. Chromatograms for DNA sequenced subcloned fragments of potential KO clones- *62*
4.6. Comparison of open reading frame (ORF) patterns and protein alignment of subcloned fragments as compared to control (WT) after sequencing of probable Smpd3 knockout clones- *63*
4.7. Characterization of Smpd3 knockout Clone 2 model- *63*
4.8. Figures
Figure 4- *65*
Figure 5- *66*
Figure 6- *68*
Figure 7- *69*
Figure 8- *70*
Figure 9- *71*
Figure 10- *72*
Figure 11- *73*
Figure 12- *74*
Figure 13- *75*
Table 1 & Figure 14- *76*
Figure 15- *77*
Figure 16- *78*
Chapter 5: Discussion- *79*
Chapter 6: Conclusion and Future Directions- *90*
Chapter 7: References- *92*

Acknowledgement

I immensely thank my almighty God for blessing me with this journey of everyday new learnings and constant feeding on knowledge which made me grow personally and professionally in many heights. I am happy and honored to have been part of this exciting research project at Dr. Murshed's laboratory which also enabled me to complete my part of objectives in the project reasonably well. Along with, I thank for all the prayers and good wishes of my near and dear ones, or this path would not have been an easy one.

Again, I whole-heartedly thank Dr. Monzur Murshed for not only being a true mentor with optimistic conviction to discover scientific truths but also for believing in the fact that each trainee of his, has an extraordinary potential in them, wherein he always made sure that all the time, the drive was enough to make me also meet my true potential in challenging times. Although we started working during the pandemic and witnessed the uncertain times together, I noticed that the quench to focus on research continued for Dr.Murshed, especially his dedication towards instructing students and building on existing studies. His excitement towards every single interesting result and data itself contributed to the positive vibes of our laboratory and motivated us through our thick and thins. I learnt a great deal about research methodologies, experimental tactics and data interpretations from the year 2020 to present and I hope that I get to read more of Murshed lab's interesting works in the years to come. Dr. Murshed's compassion and consideration towards his students is commendable. I am greatly thankful to my co-supervisor Dr. Maryam Tabrizian for her valuable advice and suggestions during the pursual of my studies. I also appreciate my other committee members Dr. Suzanne Morin, Dr. Bettina Willie and Dr. Jun Li Liu for their uplifting comments, persuading support and positive remarks for thesis completion during my committee meetings. My special thanks to Suraya Yasmine, Sadhiya, and Kim Lan Luu for always supporting me earnestly since the beginning of my master program at McGill University.

I thank happily each of my current and past colleagues in Murshed lab for their generous selves during my research work. I am grateful for the motivation received from Dr. Lina Abu Nada, and Dr. Abhinav Parashar. I specially thank Dr. Hani Salam, Kyoungmi Bak, Dr. Abeer Ahmed, Dr. Laura Capasso for their most sincere help received for my thesis completion. I give lots of credit for the kindness, moral support and translation of Abstract in French received from Dr. Craig Bryan. I heartily thank and remember all other friendly colleagues of mine, Dr. Jingjing Li, Dr. Ophelie Gourgas, Afroza Parvin, Nathan, Mayeesha, Lovely Yeasmin, Ibrahim Sankour, Nawara Osman, Sultanah Alshahrani; for being exceptionally cordial during my lab hours and lending me team support for tackling experimental problems with expert solutions.

I would also like to thank my department of experimental medicine for being always prompt on student tasks to be done for the fulfillment of this degree. My immense appreciation goes to Shriners Hospitals for Children's staff for making our workplace one of the best one could cherish for life. Thanks to the animal facility technicians Mia Esser and Louise Marineau, for amazing coordination and timely responses.

I cannot thank enough my beloved family and friends for their long-distance and extended support during the juncture. Research was truly a dream that became a reality for me through resilience and unending persuasion from my past mentors in India.

Contribution of Authors

Individual contributions to thesis are as follows:

Aishwaria Scaria: ***first;*** established inhibitor induced model for SMPD3, ***second;*** generated the *Smpd3KO* cellular models for pre-osteocytic cell-lines MLO-A5, analyzed gene expression for mineralized cultures,

Maryam Tabrizian: co-supervised the study, reviewed thesis and provided feedback.

Monzur Murshed: conceptualized, designed, and supervised the study; aided in interpretation of the data.

Hani A. Salam: reviewed and revised sections of this thesis.

Abbreviations

ALPL: alkaline phosphatase

ATP: Adenosine triphosphate

bps: base pairs

CRISPR: Clusters of regularly interspaced short palindromic repeats

Ca: Calcium

DNA: deoxyribonucleic acid

ECM: extracellular matrix

HPRT: hypoxanthine guanine phosphoribosyl transferase

HA/HAP: hydroxyapatite

KO: knockout

MGP: matrix Gla protein

MSCs: mesenchymal stem cells

MVs: matrix vesicles

NCPs: Non-collagenous proteins

nSMase: Neutral Sphingomyelinase

ORF: Open reading frame

PAM: Protospacer adjacent motif

PCR: polymerase chain reaction

Pi: inorganic phosphate

PHOSPHO1: Phosphatase orphan 1

PPi: inorganic pyrophosphate

qRT-PCR: Quantitative real-time PCR

RNA: Ribonucleic acid

SEM: Scanning electron microscopy

SMPD3: Sphingomyelin phosphodiesterase 3

WT: Wild type

Abstract

The mineralized skeleton in vertebrates protects the internal organs, helps in locomotion and eases survival in adverse external environment. Many biological processes and mechanisms act in concert to start and maintain the process of skeletal tissue mineralization, which occurs in all bones and some cartilaginous tissues, such as the hypertrophic zones of the growth plate cartilages. The existing body of literature in the field suggests that there are at least two main pathways for skeletal extracellular matrix (ECM) mineralization: Alkaline phosphatase-mediated collagen mineralization, and matrix vesicles (MVs)-mediated mineral nucleation in the bone extracellular space. The underlying mechanism of MV-mediated ECM mineralization in bone and cartilage is less studied and is yet to be elucidated clearly. In recent studies (including from our lab), the intracellular enzymes such as phosphoethanolamine/phosphocholine-phosphatase1 (PHOSPHO1) and sphingomyelin phosphodiesterase 3(SMPD3/nSMase2) have been proposed to facilitate MV-mediated mineralization. PHOSPHO1 marks its presence within MVs, and its inhibition reduced the ability of matrix vesicles to mineralize. It has been shown that SMPD3 is highly expressed in mineralizing tissues, especially during the early embryonic stages and fracture healing. Our lab confirmed the expression and essential role of SMPD3 in chondrocytes and osteoblasts using various genetically modified mouse models. In the current thesis, two approaches were used to inhibit/ablate SMPD3 activity in a pre-osteocytic MLO-A5 cell line. Firstly**,** MLO-A5 cells were treated by GW4869, a known inhibitor of SMPD3 while cultured in an osteogenic medium containing ascorbic acid and β-glycerophosphate. It was observed that the in-vitro culture when stained with calcein (binding to calcium salts), 14µM GW4869-treated group showed low mineral deposition as compared to the vehicle group. The Ca/P ratios determined from the scanning electron microscopy-energy dispersive X-ray analysis (SEM-EDX) were similar for the vehicle group (~2.43) and the treated group (~2.35), indicating the mineral

phases are the same. Secondly**,** a *Smpd3* knockout model was generated using the CRISPR-CAS9 approach. Next, the difference in ECM mineralization of knockout vs. control cells was examined. When stained with calcein (binds to calcium salts), the *Smpd3* knockout cells cultured in the osteogenic medium showed less mineral deposits as compared to control cells. Furthermore, the nature of mineral phases was similar in both samples as seen from the SEM-EDX analysis which showed Ca/P ratio ~2.1 for both the knockout and control groups. The cellular models generated will be useful to study how SMPD3 may regulate ECM mineralization.

Résumé

Le squelette minéralisé des vertébrés protège les organes internes, aide à la locomotion et facilite la survie dans un environnement externe défavorable. De nombreux processus et mécanismes biologiques agissent de concert pour initier et maintenir le processus de minéralisation du tissu squelettique, qui se produit dans tous les os et dans certains tissus cartilagineux, comme les zones hypertrophiques des cartilages de la plaque de croissance. L'ensemble de la littérateur existante dans ce domaine suggère qu'il existe au moins deux voies principales pour la minéralisation de la matrice extracellulaire (MEC) du squelette : la minéralisation du collagène médiée par la phosphatase alcaline et la nucléation minérale médiée par les vésicules de la matrice (VM) dans l'espace extracellulaire de l'os. Le mécanisme sous-jacent de la minéralisation de la MEC médiée par les VM dans l'os et le cartilage est moins étudié et doit encore être clairement élucidé. Dans des études récentes (y compris celles de notre laboratoire), les enzymes intracellulaires telles que la phosphoéthanolamine/phosphocholine-phosphatase1 (PHOSPHO1) et la sphingomyéline phosphodiestérase 3 (SMPD3/nSMase2) ont été proposées pour faciliter la minéralisation médiée par le VM. PHOSPHO1 marque sa présence dans les VM et son inhibition réduit la capacité des vésicules de la matrice à se minéraliser. Il a été démontré que SMPD3 est fortement exprimé dans les tissus minéralisateurs, en particulier pendant les premiers stades embryonnaires et la guérison des fractures. Notre laboratoire a confirmé l'expression et le rôle essentiel de SMPD3 dans les chondrocytes et les ostéoblastes en utilisant divers modèles de souris génétiquement modifiées. Dans la présente thèse, deux approches ont été utilisées pour inhiber/ ablaterl'activité de SMPD3 dans une lignée cellulaire pré-ostéocytaire MLO-A5. Premièrement, les cellules MLO-A5 ont été traitées par le GW4869, un inhibiteur connu de SMPD3, tout en étant cultivées dans un milieu ostéogénique contenant de l'acide ascorbique et du β-glycérophosphate. Il a été observé que la culture in-vitro, lorsqu'elle a été colorée avec de

la calcéine (liaison aux sels de calcium), le groupe traité par 14µM de GW4869 a montré une faible déposition minérale par rapport au groupe véhicule. Les rapports Ca/P déterminés par la microscopie électronique à balayage et l'analyse par rayons X à dispersion énergétique (SEM-EDX) étaient similaires pour le groupe véhicule (~2,43) et le groupe traité (~2,35), indiquant que les phases minérales sont les mêmes. Ensuite, un modèle Smpd3 knockout a été généré en utilisant l'approche CRISPR-CAS9. Ensuite, la différence de minéralisation de la MEC entre les cellules knock-out et les cellules témoins a été examinée. Lorsqu'elles ont été colorées avec de la calcéine (qui se lie aux sels de calcium), les cellules knockout Smpd3 cultivées dans le milieu ostéogénique ont montré moins de dépôts minéraux que les cellules témoins. De plus, la nature des phases minérales était similaire dans les deux échantillons comme le montre l'analyse SEM-EDX qui a montré un rapport Ca/P de ~2,1 pour les groupes knockout et témoin. Les modèles cellulaires générés seront utiles pour étudier comment SMPD3 peut réguler la minéralisation de l'MEC.

CHAPTER 1: INTRODUCTION AND LITERATURE REVIEW

I INTRODUCTION

CONTEXT

Life is a broad spectrum of events needing differentiation and evolutionary resistance for high grade mechanical strength. Physiological and sequential processes of formation, repair moreover enhanced strength support life's sustainability. A hardened structure is essential for such mechanical movement and durability. This strength is reached through skeletal tissues. For development, post the formation of skeletal tissues, it needs **Biomineralization**, which is one of the most common natural processes to add shape and toughness to an organism. Bios means life and mineralization means the aggregation of organic as well inorganic minerals like Calcium, Carbon, Oxygen, Nitrogen, Phosphate, Potassium, Silicon, Sodium, Magnesium, Zinc on the surface of cells and tissues.

In organisms, invertebrates and vertebrates follow a distinct course of mineralization. Calcium carbonates form the exoskeleton in Invertebrates while calcium phosphates make up most of the endoskeleton in Vertebrates. Examples of endoskeletal tissues include **Tooth**, **Cartilage** and **Bone.** Bone tissues are classified under the type of skeletal connective tissue in animals with a backbone. Ossification is the term that depicts genesis of hard tissue such as bone. Bone tissue is confined to an outer hard compact layer and an inner spongy layer with red marrow intact. Cells responsible for the formation of bone are called **Osteoblasts** while **Osteoclasts** degrade them. Bone cells arise from their progenitors' pre-osteoblasts, which are differentiated from the lineage of Mesenchymal stem cells by the activation of cell type specific **signaling factors**. **Osteocytes** are former osteoblasts present within a mineralized bone matrix that supports a network sensitive to hormonal and mechanical stimuli which harmonize the function of osteoblast and osteoclast.

Osteoblasts synthesize bone matrix, further mineralized by protein-based pathway and another extracellular vesicle mediated. Enzymatic proteins such as Alkaline phosphatase and scaffold protein collagen-I enrich the bone matrix with deposition and mineral precipitation of calcium-phosphates. Nano-sized particles like **Matrix vesicles** released from the osteoblastic membrane are a kind of extracellular vesicles which also mineralize the bone scaffold as it erupts into **hydroxyapatites** after calcium-phosphate crystals are formed. Two intracellularly active enzymes are found such as **PHOSPHO1** and **SMPD3** is supposedly expressed within MVs along with a role in its biogenesis. However, understanding is minimal in terms of MVs mediated pathway of mineralization and the correspondent role of SMPD3. So, it will be a novel factor to find and investigate the mechanism which is involved that may serve as a linking knowledge in healing bone fracture defects.

II LITERATURE REVIEW

1. Biomineralization

1. 1. Evolutionary Importance

Eukaryotic bio-mineralizing organisms stand for a majority of the Phanerozoic (current geological eon) diversity that began 541 million years ago in which plants and animals were found in abundance, and their prominent rise shifted forever both ecological dynamics and biogeochemical cycles[1,2,3]. Although biomineralization evolved many times in different eukaryotic grades, mineralized structures are not abundant in the fossil record until the terminal Ediacaran and Cambrian expansion in metazoan skeletons[2,4]. Phosphatic replacement is widespread in the Neoproterozoic and Cambrian fossil record, in addition, calcium phosphate biomineralization is rare among modern marine microeukaryotes because phosphate can be a limiting nutrient in many marine ecosystems and the energetic cost of biomineralization with a calcium phosphate phase in these environments would be prohibitively high [5,6].Even

heterotrophs in modern pelagic marine systems can be Phosphate limited because of limitation in their prey whereas phosphate biomineralization was permitted by elevated marine phosphate concentrations that were, in turn, influenced by local redox (reduction and oxidation reactions) instability associated with the prolonged ventilation of the Neoproterozoic (geologic era -1000 to 541 million years ago) oceans [4,6,7].

1.2. Comparison between invertebrate and vertebrate mineralization

The origin of biomineralization has been traced back to the late Precambrian period after tectonic activities caused a marked increase of soluble minerals in the seawater[5,8]. It is commonly believed that marine organisms first developed primitive exoskeletons made up of calcium carbonate and/or calcium phosphate minerals[3,8]. As part of the process of evolutionary adaptations, the skeletal tissues were internalized, which paved the way for the emergence of organisms with larger body sizes[3,9]. Whereas it is not clear what prompted some primitive organisms to deposit calcium phosphate instead of calcium carbonate minerals in their skeletal tissues, it is conceivable that the deposited calcium phosphate minerals supplied certain physiological advantages[9]. Indeed, it has been suggested that the presence of calcium phosphate minerals makes the skeleton more stable under acidic conditions [8,9]. In present-day invertebrates, which lack an internal skeleton, hydroxyapatite (HAP) formation has been seen on the mandibular teeth of most crustaceans, suggesting that biomineralization is widely conserved across Kingdom Animalia[4,9]. Molecular and paleontological evidence has allowed the elaboration of a timeframe for the emergence of the various vertebrate skeletal tissues[3,9]. Hyaline cartilage is ancestral to vertebrates[10] and most probably evolved earlier than vertebrates[11], while dermal and perichondrial bone, but also globular mineralized cartilage, is found in early agnathan vertebrates[12]. Cartilage mineralization in chondrichthyans mainly occurs under the form of tesserae that are small articulated units of cartilage impregnated with

apatite and are a shared derived character of this group[13]. Paleontological evidence, therefore, implies that cartilaginous fishes have lost dermal and perichondrial bone more than 400 million years ago[12]. Several genetic data were interpreted considering this evolutionary framework for skeletal tissues, however, our knowledge of chondrichthyan genomes is still scarce[14,15,16,17].

Recent studies which reassessed poor mineralization features mentioned in cartilaginous fishes [15,16,18,19,20,21,22,23]; leading to new questions on the origin and evolution of tissues mineralized in this clade and particularly in vertebrates. Distinct studies of skeletal tissues in non-tetrapods have explored a broader group of skeletal tissues unknown from an exclusive study of tetrapods[24,25]. Teleost fishes display for example a wide variety of skeletal tissues with intermediate features (e.g., hyaline, elastic, fibrous, whether mineralized or not) of what is classically associated to either bone or cartilage and for which standard characterization by histology has been proposed[25,26]. An elaborate discussion on the diversity of skeletal tissues in non-tetrapod species yet needs a deeper knowledge and comprehension of the origin, moreover, the diversity of mineralized tissues in vertebrates.

1.2.1 Ectopic calcification

The inappropriate biomineralization of soft tissues (e.g., cardiovascular tissue) is defined as ectopic calcification [27]. The factors that predispose the appearance of soft tissue calcification include an increase in the circulating calcium-phosphate product in plasma, the degree of secondary hyperparathyroidism, the magnitude of alkalosis, and local tissue injury [27]. Three major categories include (1) calcification of medium-size arteries; (2) articular or tumoral calcification; and (3) visceral calcification affecting the heart, lung, and kidney. Arterial calcification often involves the media of the vessel [27]. Such calcifications are diffuse and continuous along the vessels, which occur contrastingly to the usual discrete appearance of

calcified intimal plaques [27]. This medial calcification of the vessels may be seen first in the dorsalis pedis artery, where it appears as a ring or tube as it descends between the first and second metatarsals [27]. Other sites commonly involved are the ankles, abdominal aorta, feet, pelvis, hands and wrists [27]. Unlike its pathological counterparts, physiologic mineralization occurs in skeletal tissues, such as dentine, enamel, cementum bone, and cartilage, but these form only a small fraction of those found in the living world [27]. The inorganic components of vertebrate mineralized tissues consist of extremely small crystals, mostly with dimensions of approximately 10–20 × 5 × 5nm [27]. The crystals in dental enamel have a diameter of 40 nm and, although still too small to be clearly resolved by the optical microscope, are larger than those of bone, dentine, and cementum [27].

1.2.2 Vertebrate mineralization

Mineralization is a process of deposition of calcium phosphate crystals within a fibrous extracellular matrix (ECM)[9,28]. It is often mediated through extracellular minerals, cells and matrix vesicles[28,29]. Some associated enzymes and proteins are crucial in this process and any lack in these facilitating components can result in mineralization related disorders. For instance, in Hypophosphatasia, a heritable disease characterized by deficient activity of the tissue nonspecific isoenzyme of alkaline phosphatase (TNSALP/ALPL), may cause rickets and osteomalacia [28,29]. Importantly, during the fetal and early postnatal formation and development of skeletal tissues, e.g., bone and teeth, bio-mineralization occurs [9,29]. This is continued in the whole life during the remodeling and repair of bones [9,29]. One such mechanism is skeletal mineralization, which occurs through the deposition of mineral crystals on the extracellular matrix of a bone or cartilage [9,29]. Osteoblasts in bone, chondrocytes in cartilage, and odontoblasts, and cementocytes in teeth show mineralization in an analogous manner [9,29].

In vertebrates, biomineralization is a feature considered unique to specialized bone and tooth cells by which they promote hydroxyapatite (HAP; chemical formula) deposition on the collagen matrix (type I collagen in bone, dentin and cementum, and type X collagen in cartilage) to construct endoskeleton[9]. For many decades, the mechanisms that modulate differentiation and maturation of these specialized cells have been sought as a key to understanding bone-remodeling defects[9]. Here, we report that biomineralization is an innate ability of all mammalian cells, irrespective of cell type or maturation stage [9]. This innate biomineralization is triggered by the concomitant exposure of living cells to three indispensable elements: calcium ion, phosphoester salt, and alkaline phosphatase[9].

1.3. Mineralized tissues in vertebrates:

1.3.1. Mineralized dental tissues.

Tooth development requires the coordination of epithelial, mesenchymal, hematopoietic, and neuronal cell populations to construct a functional sensory organ. Tooth formation begins with the formation of dental organ formation[30,31]. The first stage of the dental organ is known as the 'bud stage' which results from the localized proliferation of the epithelial cells in the dental lamina. At this stage, an early signaling center directs the underlying mesenchymal cells to start their proliferation and condensation [30,32]. Tooth development begins with an invagination of the ectodermal epithelium into the surrounding mesenchyme. The epithelial bud then bifurcates and elongates to form tooth enamel after the cells in the inner enamel epithelia differentiate to ameloblasts [30,32]. The underlying dental mesenchyme later gives rise to the dental pulp (DP) and dentin-producing odontoblasts, which form dentin [30,31].

In the early dental organ, the basement membrane separating the epithelial (gives rise to ameloblasts) and mesenchymal (gives rise to odontoblasts) layers are disintegrated due to

proteolytic activities of the secreted matrix degrading enzymes[30,33]. The early signaling molecules secreted by the epithelial layer helps the differentiation of the adjacent mesenchymal cells to odontoblasts [30,33]. These cells first secrete initial collagen matrix as circumpulpal dentin which is then mineralized [30,33]. The differentiated odontoblasts also secrete signaling molecules which regulate ameloblast differentiation, and enamel formation begins on top of the mineralized dentin layer creating the enamel dentin junction [30,33].

As the tooth buds grow, it drags the surrounding cells of the dental lamina giving it the characteristic shape of a cap sitting on the top of a ball of proliferating cells. This stage of the dental organ is known as the 'cap stage' [30,33]. At the end of the cap stage, a distinct enamel organ is formed [30,33]. The enamel organ has four distinct layers: outer enamel (dental) epithelium, inner enamel epithelium, stellate reticulum, and stratum intermedium [30,33]. Through distinct structural changes caused by cell proliferation, migration and differentiation of tooth cells the developing tooth takes the shape of a 'bell' [30,33]. Once the enamel formation is complete the outer and inner epithelia migrate together to form a sheath which provides signaling cues to the underlying mesenchymal cells to differentiate into odontoblasts [33]. This results in the formation of a continuous dentin layer both in the future crown and root area of the tooth [30]. Eventually the double layered sheath in the future root area is interrupted due to apoptosis, which is followed by deposition of cementum by cementoblasts which differentiate from the follicular cells surrounding the dental organ [30,34].

Enamel:

Among all the mineralized tissues Enamel is unique in a way that mineral deposition does not require any organic scaffold[33,35]. Calcium phosphate mineral crystals are deposited on the existing mineralized dentin (circumpulpal dentin) in a 'ribbon'-like manner [33,34,35]. Mature enamel is a dead tissue devoid of any cells, which serves as a hard shell (hardest tissue in the

body) to withstand occlusal forces and forms a wall of protection for the entire tooth [33,34,35]. It is uninfluenced by any bodily changes, also not susceptible to physiologic changes and devoid of any nutritional metabolism [33,35]. During enamel synthesis various inhibitors of ECM mineralization, primarily enamel matrix proteins are arranged around the growing minerals in a way that only longitudinal growth is possible [35]. During the maturation phase ameloblasts release proteases which can remove the inhibitory proteins and crystals can thicken by accumulation of calcium phosphate minerals on the surfaces that were blocked by the inhibitors [34,35]. At the end of the maturation phase, all the ameloblasts die making it impossible to regenerate damaged enamel [33,35].

Dentin:

Odontoblasts actively produce dentin (primary dentin) throughout the process of tooth development and produce the secondary dentin in continuation with the primary dentin after root formation[30,33]. The production of dentin takes place throughout life albeit at a slower pace. New dentin is always deposited first as pre-dentin, an organic matrix composed of collagen and non-collagenous proteins[30,33]. The organic matrix of dentine is predominated by a fibrous network of type I collagen that constitutes 90% of its content [30,33]. The rest 10% of the dentin matrix is formed by non-collagenous proteins (osteocalcin, osteonectin, sialoprotein and phosphoprotein) which have been proposed to be involved in tooth mineralization [30,34,35]. The organic matrix is continuous and collectively deposited by a compact layer of odontoblasts. The mineralization of the unmineralized dentin matrix (pre-dentin) is achieved by matrix vesicles (MVs) secreted by the odontoblasts [31,34,36]. The determinants that regulate bone mineralization (see below) are known to regulate dentin mineralization.

Cementum:

Cementum, or root cementum, covers the whole root surface as a mineralized tissue. According to Denton, cementum was first shown microscopically by Fraenkel and Raschkow in 1835 and Retzius in 1836[37]. It exists fundamentally in all mammalian teeth, which fit into alveolar sockets of alveolar bone, and functions as a tooth-supporting tissue in concert with the periodontal principal fibers and alveolar bone [37]. Cementum has been primitively classified into two adjacent and overlapping layers, acellular and cellular cementum defined by the presence of absence of cementocytes[37]. Acellular cementum is thin and covers the cervical root (next to the enamel layer), while thick cellular cementum covers the apical root [37]. Both the above-mentioned types of cementum are classified with two kinds of fibers, *i.e.*, extrinsic (Sharpey's) fibers that are embedded ends of the principal fibers and intrinsic fibers are those which have fibers of cementum proper [37]. It is believed that the extrinsic fibers are secreted by fibroblasts, halfway cementoblasts and then the intrinsic fibers are secreted by cementoblasts alone [37]. Cementum is often referred to as a bone-like tissue its mineralized type I collagen scaffold, although it is mechanically softer [34,37]. As seen in bone, mineralized cementum, particularly the cellular cementum, carries embedded cells (cementocytes)[37]. As in osteocytes in bone, these cells may sense mechanical forces (e.g., occlusal force) and modulate the synthesis of cellular cementum [37]. However, unlike bone, cementum is avascular and does not undergo dynamic remodeling [37].

1.3.2. Mineralized skeletal tissues

Cartilage:

Cartilage forms the second basis of endoskeleton, which in extant jawed vertebrates includes the skull, jaws, vertebrae, gills and limb skeletons[38]. Chondroblasts, chondrocytes and

hypertrophic chondrocytes are cartilage-forming cells[38]. Skeletal bone in vertebrates grows through an endochondral ossification process regulated by an epiphyseal cartilaginous part known as the growth plate [38,39,40]. During longitudinal bone growth throughout postnatal and juvenile periods until early adulthood, chondrocytes of the growth plate continue to produce new cartilage matrices that are replaced by bone at the chondro-osseous junction (COJ), the junction between calcified and non-calcified cartilage matrices, and thereby speed up the lengthening of bones[38,40]. Articular cartilage is the highly specialized connective tissue of diarthrodial joints [38,40]. Principally functions as a smooth, lubricated surface for its articulation and aids in the transmission of loads with a low frictional coefficient. It is devoid of blood vessels, lymphatics, and nerves and is subject to a harsh biomechanical environment[38,39].

With progress in endochondral ossification, a continued supply of cartilage matrices is attained through a strictly controlled columnar proliferation and differentiation of epiphyseal chondrocytes within the growth plate[38,41]. In further steps, epiphyseal nascent chondrocytes organize into a template of eventual bone that forms a succession of resting, proliferating and hypertrophic zones[42]. The terminally differentiated chondrocytes (hypertrophic chondrocytes) get the capability of mineralizing their extracellular matrix by promoting vascular invasion at the COJ, which is a critical process for recruiting osteoblast and osteoclast progenitors, before they undergo apoptosis; growth plate cartilaginous templates are then replaced by bone matrices[43,44,45,46].

Cartilage is also present throughout the bones, spine, lungs, ears and nose. Also known as hyaline cartilage and is 2 to 4 mm thick [38,39,42]. Articular cartilage is formed of a dense extracellular matrix (ECM) with a sparse distribution of truly specialized chondrocytes, but devoid of blood vessels, nerves, or lymphatics [38,39]. They are metabolically active cells that play a unique role in the development, maintenance, and repair of the ECM [38,39]. Chondrocytes originate from mesenchymal stem cells and constitute about 2% of the total volume of articular

cartilage [38,39]. These cells in the superficial zone are flatter and smaller and have a greater density than that of the cells deeper in the matrix [38,39].

Each chondrocyte sets up a specialized microenvironment and handles the turnover of the ECM in its immediate vicinity [38,39,42]. This microenvironment traps the chondrocyte within its own matrix and so prevents any migration to adjacent areas of cartilage. Rarely do chondrocytes form cell-to-cell contacts for direct signal transduction and communication between cells[22,38,39]. They do, however, respond to a variety of stimuli, including growth factors, mechanical loads, piezoelectric forces, and hydrostatic pressures. Unfortunately, chondrocytes have limited potential for replication, a factor that contributes to the limited intrinsic healing ability of cartilage in response to injury. Chondrocyte survival depends on an optimal chemical and mechanical environment [38,39,40].

In-vivo experiments with genetically modified mice have proven that secretory factors from epiphyseal hypertrophic chondrocytes are needed to finish endochondral ossification in the growth plate[22,39,40]. Of these factors, hedgehog signaling is considered one of the key regulatory signals, since growth plate cartilage and the endochondral skeleton develop abnormally in case of its dysregulation[22,38,39].

1.4. Bone as a mineralized tissue: Cell types and development

The skeleton's successful mechanical function is determined by the organizational pattern of the mineral and organic components of bone[47]. The requirement of a tissue which is light, rigid, of high tensile strength, and not brittle is achieved by a combination of dense, compact bone and cancellous bone, reinforced at points of stress[47,48]. Intramembranous ossification is the characteristic way the flat bones of the skull and the turtle shell are formed[47,48]. During intramembranous ossification in the skull, neural crest-derived mesenchymal cells proliferate

and condense into compact nodules [47,48]. Some of these cells develop into capillaries; others change their shape to become osteoblasts, committed bone precursor cells [47]. Bone is composed of four different cell types; osteoblasts, osteocytes, osteoclasts and bone lining cells [47,48]. Osteoblasts, bone lining cells and osteoclasts are present on bone surfaces and are derived from local mesenchymal cells called progenitor cells [47,48]. Osteocytes permeate the interior of the bone and are produced from the fusion of mononuclear blood-borne precursor cells [47,48]. In long bones, lamellar bone is deposited concentrically around blood vessels to form haversian systems [47,48].

Cortical bone forms the outer casing of long bones or vertebrae and has a low surface-to-volume ratio. Eighty percent of the skeleton is cortical bone and its rigidity and density account for its shape and weight-bearing properties [47,48]. Cancellous bone, found internal to cortical bone and at the end of long bones, is composed of trabeculae separated by marrow spaces. Trabecular bone is characterized by a high surface-to-volume ratio, making it far more relevant to calcium and phosphate metabolism [9,47,48]. In the adult skeleton, bone is organized with collagen fibres arranged in parallel or concentric sheets (lamellar bone) [47,48].

Most bones have a dense rigid outer shell of compact bone, the cortex and the central medullary or cancellous zone of thin interconnecting narrow bone trabeculae [9,47]. The space in the medullary bone between trabeculae is occupied by haemopoietic bone marrow [47,48]. Woven bone is formed where bone is laid down rapidly as in fetal growth, fracture healing and in pathological states of high bone turnover in adults such as primary hyperparathyroidism [47,48]. The collagen fibres in woven bone are interlaced and randomly dispersed with hydroxyapatite crystals deposited in a disorderly manner, unlike lamellar bone where they are deposited parallel to the collagen fibres [9,47]. Bone extracellular matrix includes both mineral and organic phases. About 60% of bone net weight is inorganic material, 25% organic material and 5% water. By volume, bone forms of 36% inorganic, 36% organic and 28% water [9,47,48]. The

inorganic/mineral component comprises of calcium and phosphate in the form of needle-like or thin plates of hydroxyapatite crystals [$Ca_{10}(PO_4)_6(OH)_2$] [47,48]. These are conjugated to a small proportion of magnesium carbonate, sodium and potassium ions. The organic matrix of bone is composed of collagen and non-collagenous organic materials. Collagen makes up about 90% of the organic bone matrix. Type I collagen is the most abundant form of intrinsic collagen found in the bone that is secreted by osteoblasts. Bone is a pervasive endo-skeletal tissue that exhibits two basic mineralization patterns: compact and trabecular[47,48]. The compact mineralization pattern is continuous and smooth, whereas the trabecular pattern has many branching, rod-like struts with unmineralized regions between them.

Compact and trabecular mineralization patterns are commonly used to characterize the microstructure of bone, but they also can be applied to other vertebrate mineralized tissues, such as dentine or mineralized cartilage. Bone building cells- i.e., the induction of osteoblast differentiation was considered the essential first step of biomineralization [49,50,51]. By morphology, osteoblasts are almost indistinguishable from fibroblasts [9,47,48]. By gene expression profiles, osteoblasts are like fibroblasts. Moreover, no evidence shows that biomineralization is orchestrated by specific genes expressed in osteoblasts [52,53,54]. In this context, osteoblasts are viewed as sophisticated fibroblasts, which can be merely identified by measuring a mineralized extracellular matrix when the cells are exposed to an environment containing calcium ions, β-glycerophosphate, ascorbic acid, dexamethasone, and serum (fetal bovine serum, FBS (Fetal Bovine Serum)) for a period of 3–4 weeks [55,56]. It is now also possible to assess that calcium ion, an acyclic alkane (CnH2n+2) phosphoester salt, and alkaline phosphatase are three indispensable elements governing the biomineralization in any given somatic cell, regardless of type, origin, and maturity [9,47,48].

Osteoblasts secrete abundant collagen fibrils, non-collagenous proteins and matrix vesicles[9,48], which are small extracellular vesicles that are equipped with membrane

transporters and enzymes involved in synthesis and transport of calcium ion (Ca2+) and phosphate ion (PO43−) [9,47,48]. Most of the non-collagenous organic materials are endogenous proteins produced by bone cells. One group of non-collagenous proteins is the proteoglycans[9,47,48]. This incorporates chondroitin sulphate and heparan sulphate glycosaminoglycans. As the proteoglycans bind to collagen, they may help regulate collagen fibril diameters and may play a role in mineralization[9,47,48].

Bone is a dynamic tissue that is constantly remodeled throughout life. During fetal development, most of the skeleton develops from cartilage anlagen which is eventually resorbed and replaced with bone by a process termed endochondral ossification[9,47,48]. In contrast, bones which form the calvaria, mandible and maxilla are developed from mesenchyme by a process termed intramembranous ossification [9,47,48]. Bone modelling is the process associated with growth and reshaping of bones in childhood and adolescence. In bone modelling, longitudinal growth of long bones depends on proliferation and differentiation of cartilage cells at the growth plate, while growth in width and thickness is done by formation of bone at the periosteal surface with resorption at the endosteal surface [9,47,48]. In adults, after the epiphyses close, growth in length and endochondral bone formation cease but remodeling of bone continues. Bone remodeling must be distinguished from bone modelling [9,47,48]. Remodeling constitutes the lifelong renewal process whereby the mechanical integrity of the skeleton is preserved. It implies the continuous removal of bone (bone resorption) followed by synthesis of new bone matrix and next mineralization (bone formation) [9,47,48]. Moreover, bone remodeling is an integral part of the calcium homeostatic system.

1.5. Determinants of physiologic mineralization

1.5.1 Systemic levels of calcium and phosphate ions

The acquisition and maintenance of bone mass and strength are influenced by environmental factors, including physical activity and nutrition[57]. Among micronutrients, calcium (Ca) and inorganic phosphate (P_i) are the two main constituents of hydroxyapatite, the bone mineral that strengthens the mechanical resistance of the organic matrix [9,57]. Bone has about 99% and 80% of the body's entire supply of Ca and P, respectively [9,57]. Chemically, the structure of bone mineral implies that the extracellular levels of ionic calcium (Ca2+) and inorganic phosphate (Pi) will be two critical determinants for bone mineralization [9,57]. Data from patients and animal models of human diseases say that the reduction of systemic Pi levels with or without any alteration of the Ca2+ levels lead to osteomalacia with characteristic increase of unmineralized osteoid volume [9,57]. The Ca/P mass ratio in bone is 2.2, which is as that measured in human milk. The initial step of Ca-Pi crystal nucleation takes place within matrix vesicles that bud from the plasma membrane of osteogenic cells and migrate into the extracellular skeletal compartment [9,57]. They are endowed with a transport system that accumulates Pi inside the matrix vesicles, followed by the influx of Ca ions [9,57]. This process leads to the formation of hydroxyapatite crystal and its later association with the organic matrix collagen fibrils [9,57].

In addition to this structural role, both Ca and Pi positively influence the activity of bone-forming and bone-resorbing cells [9,57]. Pi plays a role in the maturation of osteocytes, the most abundant cells in bone. Osteocytes are implicated in bone mineralization and systemic Pi homeostasis [57]. Mutations in 25, hydroxy D3-1 α-hydroxylase (needed for functional vitamin D synthesis) or inactivating mutations in vitamin D receptor, reduce the absorption of Ca2+ and Pi in the gut[57]. Additionally, these mutations also reduce the mobilization of these ions from the bone by restricting bone resorption[57]. Although Ca2+ and Pi are both integral parts

of bone minerals, genetic experiments in mice suggest that circulating Pi may have a more prominent role in the regulation of bone mineralization[9,57].

1.5.2. Collagen scaffold:

ECM is the organic part of bone consisting of type I collagen. Two genes, *Col1a1* and *Col2a1*, encode the α1 and α2 chains of type I collagen, respectively [9]. Two α1 and one α2 chains assemble to form the collagen triple helix in the extracellular spaces of the bone microenvironment [9]. In a hierarchical fashion, these helices are first arranged axially in a staggered manner as collagen fibrils, which are then bundled together to form the collagen fibers[9]. In a healthy individual, the mineralization of the unmineralized collagen (osteoid) occurs seamlessly in continuation of the existing mineralized matrix on which the newly synthesized osteoid is deposited by the osteoblasts [9,57].

The involvement of collagen in bone mineralization came from the first electron microscopy of the mineralizing bones from newborn mice shown by Sheldon and Robinson in 1957. Although earlier studies supplied circumstantial evidence that mineral crystals are deposited within the collagen fibrils, this study first proven that there are two sites on the collagen matrix in bone where mineral deposition starts (1) at the intrafibrillar gap spaces, where the carboxy- and amino-terminal ends of two serially arranged collagen triple helices meet, and (2) interfibrillar spaces between the fibrils[9]. Since then, many studies have confirmed the critical role of collagen matrix as a scaffold for bone mineral deposition [9,57]. These include the first studies proving that collagen sponges can be mineralized in vitro, implanted collagen can mineralize in vivo, and demineralized bone collagen can be mineralized under a cell-free condition[9,57]. More recently, genetic experiments have shown that the reduction of collagen synthesis in bone results in a reduction of mineralized bone mass[9,57]. The amino acid side chains exposed at the intrafibrillar gap space and at the interfibrillar space may regulate this

process[9,57]. However, it is possible that the dense packaging of collagen molecules and their hierarchical organization, rather than the protein's primary structure, is the driving force underlying the nucleation of hydroxyapatite[9,57]. Indeed, one theory tries to explain the mineralization of bone ECM by the size-exclusion properties of the collagen scaffold[9,57].

1.5.3 Inhibitors:

Matrix Gla protein

Matrix GLA protein (MGP), a γ-carboxyglutamic acid (GLA)–rich, vitamin K–dependent and apatite-binding protein, is a regulator of hypertrophic cartilage mineralization during development [39,57]. However, MGP is produced by both hypertrophic and immature chondrocytes, pointing out that MGP's role in mineralization is cell stage–dependent and also MGP may function other roles in immature cells[39,57]. All members of the family contain glutamyl groups, some of which are posttranslationally modified by a vitamin K–dependent γ-carboxylase into γ-carboxyglutamic acid (GLA) residues [39,57]. In both MGP and osteocalcin, the GLA residues promote binding of calcium and phosphate ions[39,57]. A combination of charge and lattice geometry eases adsorption of calcium atoms into the hydroxyapatite crystals[39,57]. During development, MGP and osteocalcin gets accumulated in mineralized cartilage and bone[39,57]. Such findings have led to the long-held view that MGP and osteocalcin must provide important regulatory roles in the mineralization of skeletal and dental tissues[39,57]. Pharmacological and genetic approaches have been used to gain insights into these regulatory roles. For example, treatment of pregnant rats with the vitamin K antagonist, warfarin, reduces GLA residue synthesis in the fetus and newborn and causes severe skeletal malformations [39,57]. These defects include disorganization and excessive mineralization of growth plate and nasal septum cartilages, precocious closure of the growth plate, growth retardation, and abnormalities in, or absence of, ossification centers[57]. A similar prenatal exposure to warfarin is associated with embryopathy and skeletal defects in humans[57]. Recent genetic studies have

shown that mice lacking a functional MGP gene is practical, but show increased calcification of growth plate cartilage, short stature, osteopenia, and fractures[57]. The MGP-deficient mice die around two months of age due to excessive abnormal calcification of their arteries leading to blood vessel rupture. In a related study, ablation of the osteocalcin gene was also found to be compatible with life[53,57].

Mutations in the human MGP gene cause Keutel syndrome, which is a disorder characterized through excessive cartilage calcification[57]. The above pharmacological and genetic studies have led to a conclusion that, despite their abundance in skeletal tissues and their ability to bind calcium and apatite, MGP and osteocalcin may serve as inhibitors of cartilage mineralization and bone formation, respectively [39,57]. First, the protein is not only present in the mineralizing zone of the growth cartilage but is also present in articular cartilage and certain non-skeletal tissues[9,39,57]. Yet, interference with MGP function in vivo by warfarin treatment or ablation of the MGP gene does not lead to widespread random mineralization[9,39,57]. Excessive mineralization is seen only at specific sites, such as the growth cartilage and arteries[9,57]. This finding raises the possibility that MGP function in mineralization may depend on the stage of development of the responding cells or the nature of the responding cells [39,57].

Pyrophosphates:

Inorganic pyrophosphate has long been known as a by-product of many intracellular biosynthetic reactions and was first identified as a key endogenous inhibitor of biomineralization in the 1960s[57,58]. The major source of pyrophosphate is extracellular ATP, which is released from cells in a controlled manner. Once released, ATP can be rapidly hydrolyzed by ecto-nucleotide pyrophosphatase/phosphodiesterases to produce pyrophosphate [9,57,58]. The main action of pyrophosphate is to directly inhibit hydroxyapatite formation thereby acting as a physiological ‘water-softener’[9,57,58]. Evidence suggests pyrophosphate

may also act as a signaling molecule to influence gene expression and regulate its own production and breakdown [9,57,58]. Pyrophosphate and longer chain polyphosphates can be synthesized under some circumstances, particularly by bacteria and non-mammalian organisms, pyrophosphate is not thought to be produced directly by mammalian cells [9,57,58]. Instead, it is generated by the hydrolysis of the phosphodiester bond in nucleotide triphosphates such as ATP or UTP[58]. As such it is a metabolic by-product for many intracellular biochemical reactions and extracellular signaling cascades [58]. It was the pioneering work of Fleisch and colleagues in the 1960s that noticed the ability of pyrophosphate to inhibit biomineralization[9,57,58]. They discovered that pyrophosphate potently antagonizes the ability of calcium to crystallize with phosphate to form hydroxyapatite (Ca10(PO4)(OH2))[58]. Pyrophosphate also binds strongly to the surface of hydroxyapatite crystals and blocks their ability to act as a nucleator for mineralization, preventing further crystal growth[58]. This base work helped to set up the concept that pyrophosphate is the body's own 'water softener' which acts to prevent harmful soft tissue calcification and regulate bone mineralization [58]. Later studies using 32P-labelled pyrophosphate in dogs enabled the kinetics of pyrophosphate production and elimination to be examined[9,58]. This work suggested that the daily turnover of extracellular pyrophosphate in an adult human might be in the range 100mg/day, an exceedingly small amount compared with the many grams likely to be generated intracellularly during biosynthetic reactions[9,58]. Pyrophosphate is found in mineralized tissues (e.g., teeth and bone) at concentrations being approximately 0.5% of the total phosphate content[9,58]. The intracellular concentrations have been difficult to find, not least because of compartmentalization, but might be at least tenfold lower than that of inorganic phosphate[57,58].

1.5.4 Intracellular enzymes:

PHOSPHO1 (Phosphatase orphan 1)

Phosphoethanolamine or phosphocholine phosphatase has been implicated in generating inorganic phosphate (Pi) for matrix mineralization[59,60]. These metabolizes phospholipids and/or associated metabolites[61,62] wherein the deficiency of PHOSPHO1 in mice had caused similar bone mineralization defects as seen in *fro*/*fro* mice[63]. Previous study on PHOSPHO1 mRNA expression during embryonic development in the chick; whole-mount in situ hybridization showed PHOSPHO1 expression has occurred prior to E6.5 and was initially restricted to the bone collar within the mid-shaft of the diaphysis of long bones but by E11.5 expression was observed over the entire length of the diaphysis [9,59,60].

The Alcian blue/ alizarin red staining also revealed that PHOSPHO1 expression noted in the primary regions of ossification preceded the deposition of minerals, which suggested its involvement in the initial events of mineral formation [9,57,60]. Expression of PHOSPHO1, like TNAP activity, is found to be up regulated in MVs isolated from chondrocytes induced to differentiate by adding ascorbic acid[57,60]. Henceforth, both enzymes may be regulated by similar mechanisms [9,57,60]. By this route of investigation, for the first-time direct evidence has been built up that PHOSPHO1 is present in MVs, and its developmental expression pattern is also consistent with a role in the initial stages of matrix mineralization [9,57,60].

SMPD3 (Sphingomyelin phosphodiesterase 3 /neutral sphingomyelinase 2):

SMPD3 is a cell membrane bound protein and a lipid-metabolizing enzyme expressed highly in the brain, cartilage, and bone. It is noted that among the acid, basic, and neutral sphingomyelinases, only SMPD3 deficiency has led to impaired mineralization in skeletal tissues[9,64,65]. A bioactive lipid molecule such as ceramide and a nutrient phosphocholine are the metabolites when sphingomyelin present in the cell membrane is cleaved by SMPD3. Past

data from the research of genetically altered mouse models indicate SMPD3 activity during their embryonic development, which has shown an impact on the normal skeletogenesis[9,57,66,67,68]. One of the two models that lacked SMPD3, *fro*/*fro,* carried a chemically induced deletion including segment of intron 8 and most of exon 9 of the *Smpd3* gene, while another model (*Smpd3*$^{-/-}$) was a resultant of a conventional gene-targeted approach[9,57,66,67,68].

The *fro* mutation eliminates the enzymatic activity of SMPD3, though its membrane localization is still unaffected; however, the mineralization defect affects intramembranous as well as endochondral bones, and an abnormal delay in apoptosis of the hypertrophic chondrocytes at the preliminary stages of skeletal development are known as hallmarks of skeletal phenotypes in *fro*/*fro* mice [9,57,66,67,68]. Recently, it has been noted and inferred that SMPD3 activity in both chondrocytes and osteoblasts are essential for normal bone development. Poor skeletal mineralization phenotype in *fro*/*fro* mice is seen devoid of any alterations of the homeostasis of Ca^{2+}, P_i, and PP_i [9,68]. This suggested that the loss of SMPD3 function affects ECM mineralization through a novel, yet unknown, mechanism [9,66,67].

As noted above, SMPD3 cleaves sphingomyelin into by-products of several ceramides that regulate cell functions at large and this SMPD3 activity also releases an essential nutrient, phosphocholine [9,57,66,68]. Also, the role of ceramide is recorded well in terms regulating apoptosis [9], yet it is vague about if both ceramide and phosphocholine or only one of these metabolites is critical for skeletal tissue mineralization. Interestingly, gene knockout experiments decreasing ceramide biosynthesis via an alternative pathway without involving SMPD3 activity did not show any ECM mineralization defects [69]. Two conclusions were drawn from these findings: it is possible that the ceramides produced in the two pathways may contribute to different pools with distinct cellular functions; alternatively, the ceramides may not have a role in bone mineralization [9]. Currently, there is no experimental data available

suggesting the involvement of ceramide in ECM mineralization, but the importance of phosphocholine in this process has been convincingly proved through animal experiments[63,65]. Phosphocholine, a metabolite, generated from sphingomyelin by SMPD3, or from dietary choline via two isoforms of choline kinases, can be cleaved by PHOSPHO1, an intracellular enzyme with phosphatase activity [9,57,66,68].

1.6. Revisiting the matrix vesicle theory

In bone, primary mineralization is constituted with two distinct phases: matrix vesicle-mediated mineralization and collagen mineralization. During the matrix vesicle-mediated mineralization process, osteoblasts secrete matrix vesicle on which the membrane transporters and enzymes involved in mineralization are equipped[9,36]. The theory behind matrix vesicle-mediated mineralization sustains that the mineralization processes are under the biological control of osteoblasts, by mediating the regulation of membrane transporters/ enzymes and surrounding extracellular organic materials [9,36,70]. Accumulated knowledge of the ultrastructure and biological activities of membrane transporters/enzymes supports the postulation that the cellular mechanisms of matrix vesicle-mediated mineralization are essential for mineralization in bone [9,36,70].

Bone mineralization initiates inside matrix vesicles. Matrix vesicles are small extracellular vesicles enveloped by a plasma membrane secreted by osteoblasts [9,36,70]. Matrix vesicles equip several membrane transporters and enzymes on their plasma membranes and in their interior, supplying a nurturing microenvironment for calcium phosphate nucleation and next crystal growth. Mineralization begins when a crystalline calcium phosphate, i.e., hydroxyapatite [Ca10(PO4)6(OH)2], appears inside the matrix vesicles, growing and eventually breaking through the plasma membrane of matrix vesicles to form mineralized nodules such as

calcifying globules. Under transmission electron microscopy (TEM), mineralized nodules are seen as the radially assembled globular structures of hydroxyapatite crystals featuring small, ribbon-like structure profile approximately 25 nm wide, 10 nm high and 50 nm long [9,36,70]. The plasma membranes of matrix vesicles are rich in acidic phospholipids such as phosphatidylserine and phosphatidylinositol, which have high affinity for Ca2+ due to phosphate residues[9,36]. Phosphatidylserine has a particularly high affinity for Ca2+ and is assumed to produce a stable calcium phosphate-phospholipid complex associated with the inner leaflet of the vesicle's membrane [9,36,70]. The possibility of such complexes may play a vital role in crystal nucleation has been noted[9,36]. However, the electron diffraction of freeze-substitution and cytochemical calcium detection methods such as κ-pyroantimonate combined with energy-dispersive X-ray spectroscopy showed immature calcium phosphates associated with the vesicles' plasma membranes as non-crystalline structures holding calcium and phosphate [9,36]. Thus, the early phases of calcium phosphate nucleation inside the matrix vesicles may be originally amorphous, thereafter chronologically becoming mature crystalline structures, i.e., hydroxyapatite, in a later stage [9,36,70].

Calcium phosphate crystals formed inside matrix vesicles can thereafter grow through the influx of Ca2+ and PO4 3- from extracellular fluid, by the membrane transporters and enzymes. Inside the matrix vesicle, "needle-shaped" crystalline calcium phosphates form a stellate assembly, grow in all direction, and then, come out of the vesicles penetrating the plasma membrane to form mineralized nodules, also referred to as calcifying globules [9,36,70].

1.7. In vitro cell culture models depict bone mineralization

1.7.1. Secondary cell lines:

MC3T3-E1

MC3T3-E1 cells, first explained in 1983, have a fibroblastic shape and their size is about 20–50 μm in diameter[71,72,73]. These cells are derived from murine calvaria and expresses high alkaline phosphatase activity in the resting state, while too low in their growing state [71,72]. However, enzyme activity is a hundredfold higher when it becomes confluent. These are osteogenic cell lines that can differentiate into osteoblasts and mimics mineralization in-vitro[71]. Therefore, they can be considered as pre-osteoblastic cell lines. As previously seen, calcified bone tissue was formed in MC3T3-E 1 cultures by a process closely resembling that seen in intramembranous osteogenesis in vivo [71,72].

MLO-A5

MLO-A5 cell line is a representative of the post osteoblastic and pre-osteocytic cells[48,74]. At such a differentiating stage these cells can be also called young 'osteocytes' [48,74]. These cells are large, over 100 μm, express markers of the late osteoblast such as extremely high alkaline phosphatase, bone sialoprotein, PTH type 1 receptors, and osteocalcin, and rapidly mineralize in sheets, not nodules [48,74]. Another advantage of these secondary cells is the ability to mineralize without the addition of β-glycerophosphate (BGP) and Ascorbic acid [48,74]. Comparatively, with respect to MC3T3 cells, MLO-A5 cells are known to mineralize matrix faster in culture than other cell types with added β-glycerophosphate (BGP) and Ascorbic acid [48,74]. Earlier studies suggested MLO-A5 cells were found to mineralize within 7-8 days in the absence of β-GP and within 2-3 days with the addition of β-GP [48,74].

In culture, these cells start to express markers of mature osteocytes such as E11/gp38/pdpn as they generate cell processes. PTH and mechanical load decreases Sclerostin expression in these

cells, while Bone Morphogenetic Protein increases it [48,74]. MLO-A5 cells have been used to study the osteoblast to osteocyte differentiation process, the mineralization process, and the effects of mechanical loading on biomineralization [48,74].

1.8. Extracellular matrix proteins and mineral deposition

Research is constant in identifying the initiation of mineral deposition to start in different physiologically and abnormally calcified tissues [9,57,71,75]. Information is in plenty on the mineral and matrix components in bones and teeth, in the exoskeletons of invertebrates, and in dystrophic deposits such as those in atherosclerotic plaques, salivary and kidney stones, calcific deposits in osteoarthritis, etc. [9,57,71]. It also includes detailed characterization of the physical and chemical composition of the mineral and matrix, and details on the gene localization and regulation of gene expression for the major and minor protein constituents, but the precise reason that mineral deposition occurs in some tissues and not in others stays unclear [9,57,71]. However, there are some generally accepted facts about the formation of physiologic minerals, and some molecules essential for physiologic calcification in the relevant tissues [9,57,71,75].

In normal bone physiology, extracellular bone matrix is secreted by osteoblasts as the type I tropocollagen [9,57,71]. The first matrix produced is rapidly degraded by osteoclasts and replaced by organized matrix. This tropocollagen is deposited and cross linked in dense lamellae aligned in one direction, ~2-μm thick, after which orientation shifts ~90° to form a new lamella [9,57,71,75]. This matrix is mineralized by deposition of hydroxyapatite, which, as discussed below, requires massive local phosphate production that requires alkaline phosphatase activity, passive calcium transport, and removal of acid. Specifically, phosphate production under osteoblasts, supported by massive alkaline phosphatase expression and secretion of phosphatase substrates, is needed for mineral deposition [9,57,71,75]. Alkaline phosphatase is also

essential for pyrophosphate degradation; if not degraded, this is a mineralization inhibitor[9,57,71]. If phosphate production ceases, as in lethal forms of hypophosphatasia, bone is not mineralized, and pyrophosphate accumulates. In the following sections, we will address bone formation in vitro, growth factors for bone cells including bone morphogenetic proteins (BMP) and transforming growth factor-β (TGF-β) family signals, and initiation of bone differentiation; also, an activin receptor 1 defects with uncontrollable bone formation [9,57,71,75].

Physiologic mineral deposition-i.e., the formation of mineral in an organized fashion in shells, in teeth and in bones does not occur without a matrix [57,71]. The matrix supplies an oriented support for mineral deposition and may participate directly in the mineralization process by serving as a nucleator, or holding and orienting ions which become incorporated into the mineral crystals [57,71]. It is also well accepted that the matrix is not the same in all mineralized tissues [9,57,71]. Even in the vertebrates where type I collagen is the predominant matrix part of dentin, cementum, and bone; the calcified cartilage matrix is distinct, having types 11, IX and X collagen as well as proteoglycans; and the enamel matrix is even more unique [9,57,71]. The matrices which have type I collagen are also distinct, consider for example the unique dentin phosphoproteins, dentin phosphophoryn, dentin sialoprotein, and dentin matrix protein I, which do not exist in bone [9,57,71].

It is also well proven that extracellular matrix vesicles, may not always be the site of initial mineral deposition [9,57,71]. In turkey tendon and in certain cell culture systems, matrix vesicle and collagen mineralization, distinct in site, start simultaneously. In other tissues sulphate-rich proteins, perhaps bone sialoprotein or proteoglycans, appear to be sites of initial mineralization. many but not all invertebrates, and in enamel, there are no extracellular matrix vesicles [9,57,71]. Thus, there must be other means of initiating calcification besides accumulating ions in a protected environment like the vesicles [9,57,71]. Finally, it is accepted that in vitro, and by analogy in vivo, matrix proteins can start mineralization and regulate the growth, proliferation,

or agglomeration of mineral crystals [9,57,71,76]. They may do this by stabilizing crystal nuclei[9,71,76]. They may bind to one or more crystal surfaces as the crystals grow, regulating the shape and size of the crystals, as has been shown for the mollusk shell proteins, fibronectin,and dentin phosphophoryn in the case of octacalcium phosphate and apatite formation [9,57,71]. By binding to growth sites on the crystals, they may prevent or retard crystal proliferation, as exemplified by osteopontin and proteoglycan aggregate [9,57,71]. Immobilized osteocalcin and Bone sialoprotein (BSP) have been reported to act as nucleators [9,57,71].

The ECM is principally composed of water, collagen, and proteoglycans, with other non-collagenous proteins (NCPs) and glycoproteins recorded with lower expression[9,57,71,75]. Together, these components help to keep water within the ECM, which is critical to keep its unique mechanical properties[9,57,71]. Along with collagen fiber ultrastructure and ECM, chondrocytes contribute to the various zones of articular cartilage [9,57,71]. So, the matrix consists of several distinct regions based on proximity to the chondrocytes, composition, and collagen fibril diameter and organization [9,57,71]. The pericellular matrix is a thin layer next to the cell membrane, and it fully surrounds the chondrocyte [9,57,71]. It has mainly proteoglycans, as well as glycoproteins and other NCPs and this matrix region may have a functional role to initiate signal transduction within cartilage with load bearing[9,57]. The territorial matrix surrounds the pericellular matrix; it is composed mostly of fine collagen fibrils, forming a basketlike network around the cells [9,57,71]. This region is thicker than the pericellular matrix, and it has been proposed that the territorial matrix may protect the cartilage cells against mechanical stresses and may contribute to the resiliency of the articular cartilage structure and its ability to withstand large loads [9,57,71]. The interterritorial region is the largest of the 3 matrix regions; it contributes most to the biomechanical properties of articular cartilage [9,57,71]. This region is characterized by the randomly oriented bundles of large collagen fibrils, arranged parallel to

the surface of the superficial zone, obliquely in the middle zone, and perpendicular to the joint surface in the deep zone [9,57,71]. Proteoglycans are abundant in the interterritorial zone.

1.9. CRISPR/Cas9 as a tool for DNA modification

Clustered regularly interspaced short palindromic repeats/CRISPR-associated protein 9 (CRISPR/Cas9) technology has been appearing in the molecular biology research spotlight[77,78]. As a game-changing player in genome editing, this technology has revolutionized animal research, including medical research and human gene therapy as well as plant science research, particularly for crop improvement[77,78]. One of the most common applications of CRISPR/Cas9 is to generate genetic knock-out mutants[77,78]. Also, several multiplex genome editing approaches utilizing CRISPR/Cas9 have been developed[77,78]. Compared with genetic crossing, CRISPR/Cas9 multi-gene targeting can greatly shorten the process of higher-order mutant generation and screening, which is especially useful to characterize genes that require longer growth time[77,78]. Moreover, CRISPR/Cas9 makes it possible to knock out genes when null T-DNA mutants are not available or are genetically linked. Because of these advantages, CRISPR/Cas9 is becoming an ideal and indispensable tool to perform functional studies [77,78]. Hence, CRISPR -associated protein 9 (Cas9) genome editing system has become a versatile tool to perform precise gene targeting and mutations including gene insertions/deletions, gene replacements, and single base pair conversions [77,78].

1.9.1. Adaptation in predecessor bacteria, the original mechanism

CRISPR/Cas9 was first discovered as an adaptive immune defense system in bacterial cells as a mechanism to ward off foreign DNA[77,79,80]. Clustered regularly interspaced short palindromic repeats (CRISPR) and their associated *cas* genes serve as a prokaryotic 'adaptive' immune system, protecting against foreign DNA elements such as bacteriophages and plasmids[77,78]. This immunity is conferred by site-specific cleavage of the invading DNA element, targeted by short DNA 'spacers' present in the CRISPR array and homologous to the invading sequence [77,78]. The remarkable ability to acquire new specificities by incorporating more spacers is what sets CRISPR-Cas systems apart from other, analogous, microbial defense systems [77,78]. Genetic manipulation of the arrays has also enabled their use as targeted genome editing tools, a field which has exploded in 2013[77,78]. However, the process of natural spacer acquisition is still enigmatic, demonstrated in the laboratory in only a few systems. In contrast, acquisition of spacers is clearly occurring in natural populations, which diverge considerably at their CRISPR loci [77,78].

Streptococcus thermophilus possesses two active type II-A CRISPR systems (CR1 and CR3) and is by far the best-studied model of natural spacer acquisition. This is due, at least partly, to the negligible frequency of phage resistance by mechanisms other than CRISPR-Cas[77,78]. Bacteriophage-insensitive mutants (BIMs) in this bacterial species are almost always associated with spacer acquisition in either the CR1 and/or CR3 arrays[77,78]. The process of getting CRISPR-based immunity against phages in this system requires phage infection of the host cell and concomitant exposure to the phage double-stranded DNA genome followed by spacer acquisition (adaptation), expression and maturation of the newly acquired spacer to generate 'targeting' crRNA molecules (maturation) and, only then, cleavage of the invading DNA (interference)[77,78]. It can be unimaginable of all these steps occurring before the accumulation of lethal damage to the cell from an invading virulent phage [77,78].

1.9.2. Manipulated and engineered for eukaryotic gene editing

The CRISPR/Cas9 machinery, when adapted for genome editing, consists of two parts: a guide RNA (gRNA) and the Cas9 endonuclease [77,78,81]. A gRNA is 20 nucleotides (nt) long which is a high-end gene-specific sequence[77,82]. Each gRNA is complementary and binds to a specific target DNA sequence that ends with a short DNA sequence, known as the protospacer adjacent motif (PAM), which is often "NGG" [77,78,81]. The PAM region is critical for Cas9 binding and 3 base pairs (bp) are found downstream of the cleavage site of the Cas9 endonuclease[77]. Adjacent to the 3′ end of the 20 nt gRNA is an ∼80 nt long gRNA scaffold sequence that is necessary for Cas9 binding[77,83]. Once the gRNA-Cas9 complex forms, Cas9 makes a double-strand cut exactly 3 bp before the PAM sequence[84]. The break site is restored by non-homologous end joining (NHEJ), often error-prone and causes insertion or deletion (indel) mutations at the cut site[77,78,81]. These indel mutations lead to frame-shift mutations, affecting protein translation and thereby disrupting a gene's function [77,78,81].

Several publicly available web-based tools such as E-CRISP, CHOPCHOP, Tefor, and CRISPR-P 2.0, are used for gRNA design[77,78,81]. The design tools supply a list of possible gRNA sequences and rank them by their targeting scores for any gene of interest[85]. Depending on the gRNA sequence chosen, potential gRNA picks contain zero to many potential off-target sites with different off-target scores. It is noteworthy that the specificity of a gRNA sequence is mainly determined by the 8–12 nt gRNA sequence (i.e., the seed region) next to the PAM sequence, also known as the PAM-proximal region[77,78,81]. As the structure of the RNA–DNA heteroduplex in the PAM-distal region is more flexible than the PAM-proximal region, the proximal region is nearly intolerable to any mismatches compared to the distal region[79,83]. Knowing the specificity of a gRNA sequence also helps to evaluate potential off-target effects, since off-target effects are less likely to occur when mismatches appear in the seed region[77,78,81].

The gRNA design websites also display other features, including locations of each gRNA, its GC content, restriction enzyme (RE) sites within the gRNA sequence, potential off-target genes, and the corresponding off-target scores[77,78,81]. Generally, one should select gRNA(s) that target the 5′ region of a gene to ensure that the translation of a functional protein is stopped as early as possible. Also, functional gRNA(s) often has 40–60% GC content to increase its binding affinity with the Cas9 protein[86]. Besides using gRNA design tools, several other criteria for gRNA(s) choice should also be taken into consideration. One study found that high mutagenesis frequency is associated with having a "T" at position 3 and/or position 6, as well as a "C" at position 20 of a gRNA sequence, while having an "A" at position 20 lowered the gRNA targeting rate[87]. Moreover, gRNAs ending with "GG" can improve Cas9 enzyme activity up to 10-fold compared with gRNAs that ended with "AG" or "GA"[88]. Another study found that having a "G" next to the PAM sequence resulted in higher mutagenesis rates *in vitro*[87]. Furthermore, a gRNA that has four or more consecutive "T" nucleotides should be avoided, as such sequences can be recognized as a transcription stop site[89].

In fact, nucleotide compositions of a gRNA at distinct positions can influence the binding affinity and the structure of the Cas9-gRNA-DNA complex[90]. Further analysis found that for a Cas9-gRNA-DNA to form a stable secondary structure, base-pairing rules between an individual a gRNA-gRNA scaffold have been established: gRNA-gRNA scaffold should have less than 12 total base-pairings, a gRNA-gRNA scaffold should have less than 7 consecutive base-pairings, and internal gRNA base-pairings should be less than 6[78,91]. Therefore, choosing gRNA(s) that meet these secondary structure criteria can improve gene editing efficiency[77,78,81].

1.10. Figures (see below)

Figure 1

A

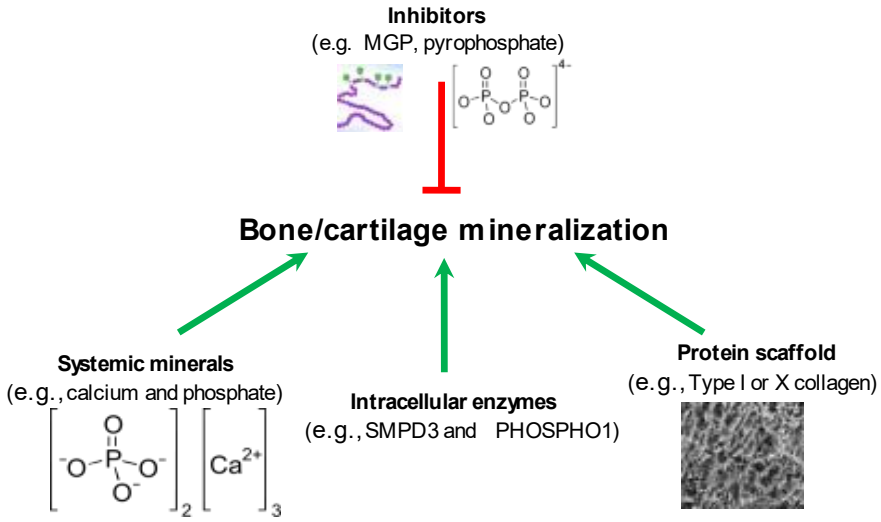

Figure 1A. Schematic representation for key regulators in Skeletal mineralization. Systemic minerals such calcium and phosphorous, intracellular enzymes such as SMPD3 and PHOSPHO1 and protein scaffolds such as Type I or X among others are positive regulators of bone and cartilage mineralization (green arrows). On the other hand, mineralization is inhibited by various proteins, molecules or enzymes such as Matrix gla protein (MGP) and pyrophosphate (red line).

B

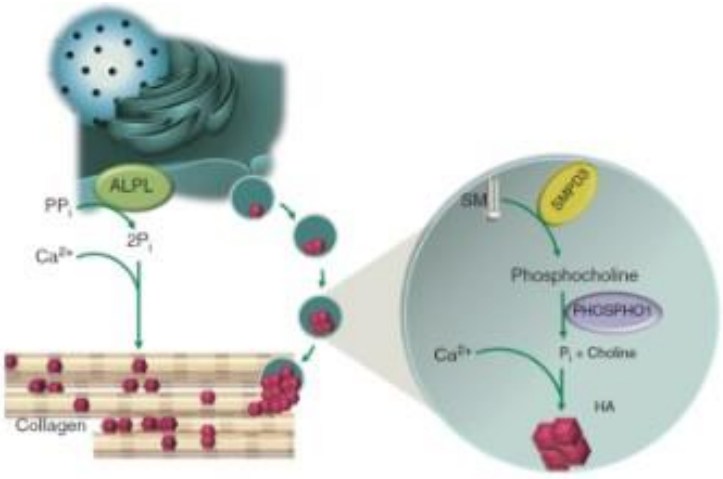

Figure 1B. Schematic representation demonstrating two enzymatic pathways of calcium phosphate-based mineralization in bone and cartilage. The alkaline phosphatase pathway is well-known, whereas the matrix vesicle pathway is less well-defined. Alkaline phosphatase, a cell-membrane enzyme phosphorylates extracellular inorganic pyrophosphate (Ppi). Calcium ions, when added to the phosphate complex leads to precipitation on the collagen fibers. Another possible pathway could be mediated via matrix vesicles that detach from the cell membrane. SMPD3 cleaves sphingomyelin to produce phosphocholine which is cleaved by PHOSPHO1 to Choline and inorganic phosphorous which combines with calcium to produce hydorxyapetite crystals. **Ref:-(**Monzur Murshed, review, Cold Spring Harb Perspect Med. 2018 Dec; 8(12): a031229. doi: 10.1101/cshperspect .a031229)

Figure 2

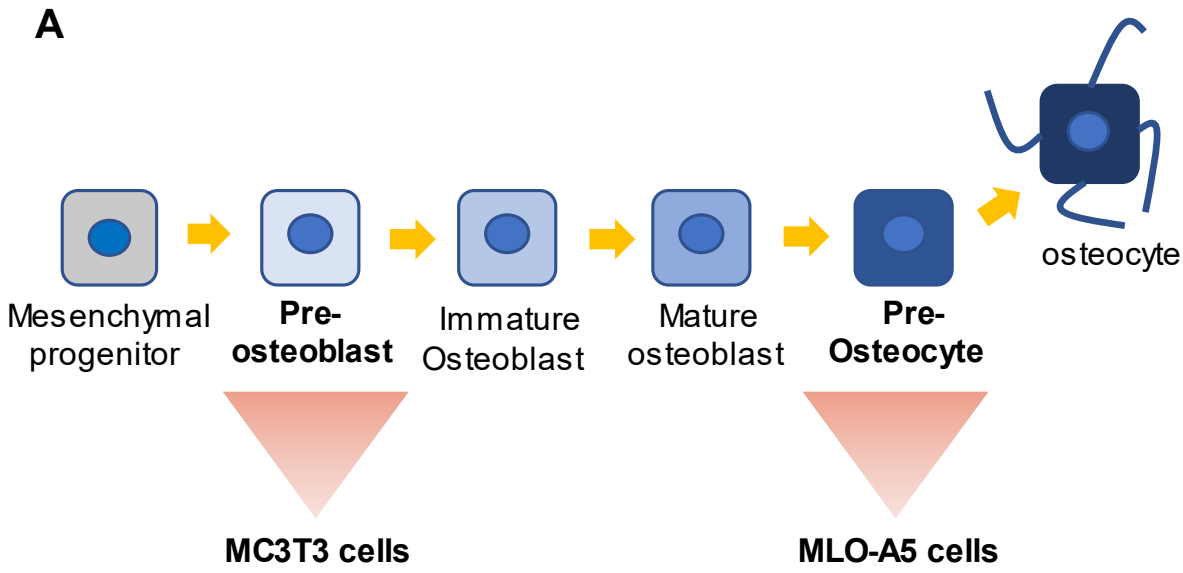

Figure 2. A. Schematic diagram showing the differentiation stages of osteoblasts. Mesenchymal progenitor cells are pre-osteoblastic cells that mature into osteoblasts that become osteocytes. MC3T3 cells mimic pre-osteoblastic cells, whereas MLOA5 cells mimic pre-osteocytes.

Figure 3

A

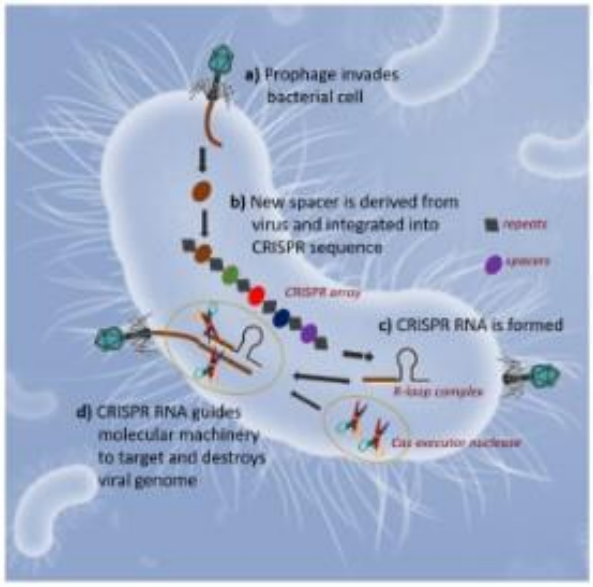

Figure 3. A. CRISPR mechanism in bacteria, (Ref: Vilela, Alice. 2021)
Bacterial survival against invasion by bacteriophages depends on storing genetic information which is integrated in the CRISPR locus against secondary attacks. Spacer DNAs, derived from the virus, are part of the CRISPR DNA sequence which is transcribed during a secondary attack to RNA that forms a complex with CAS9. This complex is complimentary to the bacteriophage injected DNA and destroys it.

B

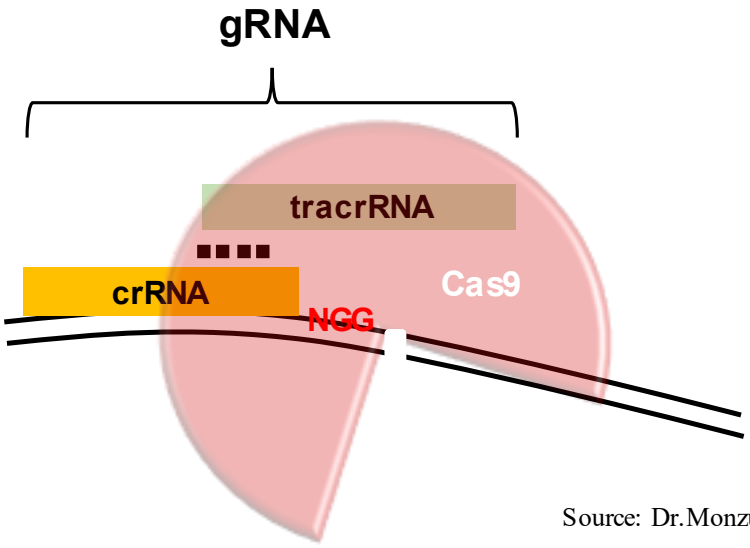

Source: Dr.Monzur Murshed

Figure 3. B. CRISPR CAS-9 system engineered for Eukaryotes
The main two components of the CRISPR CAS-9 system are: guide RNA and Cas9 protein. gRNA consists of, contiguously working, transactivating RNA (tracrRNA) and CRISPR RNA (crRNA) which recognizes the site of interest in a gene sequence. TracrRNA recruits a Cas 9 nuclease and forms a complex with gRNA creating a double-stranded break after the protospacer adjacent motif (PAM) sequence (NGG-where N can be any nucleotide). This break occurs at a specific gene region which makes the open-reading frame non-functional for the gene-specific proteins, therefore preventing their transcription and translation.

CHAPTER 2: OBJECTIVES

The following hypothesis and objectives are under my thesis research project:

Hypothesis I

Inactivation of SMPD3 through MLO-A5 cell line models generated to suppress enzyme expression by pharmacologic inhibitor treatment and knocking-out Smpd3 using CRISPR CAS-9 approach will result in poorly mineralized in-vitro pre-osteocytic culture.

Aim:

To study the regulation of bone mineralization in SMPD3 deficient MLO-A5 pre-osteocytic cell culture models.

Objective 1:

Generation of SMPD3-deficient MLO-A5 cell line pharmacologically and a genetic knockout using CRISPR/Cas9-based approach along with characterization of their in-vitro mineralization properties.

Rationale:

We have used pre-osteocytic (MLO-A5) cell lines to treat pharmacologically, a method for which we have used GW4869 a known inhibitor to SMPD3 enzyme, and it is useful to analyze mineralization aspects after the culture treatment along with differentiation inducers such as Ascorbic acid and Beta glycerophosphate to supply calcium-phosphates in-vitro.

Also, the strategy to knockout the expression of *Smpd3* gene in these cells is done using the CRISPR/Cas9-mediated targeted deletion. Considering that SMPD3 is expressed in bone forming cells that play important roles in bone mineralization; we decided to use MLO-A5 pre-osteocytes. These cells have been used successfully to study in-vitro bone ECM mineralization.

Whereas the *Smpd3* ablation in the proposed skeletal cells would allow future experiments to determine if there is any secretion of MVs and/or MVs mediated mineralization have/has altered in the absence of SMPD3 enzymatic activity. Further, this model can serve as a useful tool to characterize and investigate the role of Matrix vesicles in the pathway of bone mineralization.

CHAPTER 3: METHODS WITH MATERIALS

3.1 Treatment of MLO-A5 Cell Line with GW4869

Cells were seeded on 4-well culture plate to achieve confluency of 0.8×10^6 cells/well culture plate. For inhibition of Sphingomyelinase-2 /SMPD3, 5% Methanosulphonic acid (MSA) to solubilize 1.5mM GW4869 (Sigma) into a series of concentrations i.e.12µM, 13µM, 14µM incubated for 10 minutes at 37°C under 5% CO2 in a humidified incubator; these were used with culture media-[alpha minimal essential medium (Gibco, Thermofisher) supplemented with 10% fetal bovine serum (Hyclone, GE Life sciences) and 100 U/ml of penicillin-streptomycin] mixed with differentiation inducers: 100 µg/ml Ascorbic acid and 5 mM β-glycerophosphate (BGP), then incubated for 30 minutes at 37°C, further treatment is given to pre-osteocytic cell-line MLO-A5 cells every 48 hours for six days. Vehicle group was with cells cultured with culture media + 5% MSA (1.5mM) + differentiation inducers: 100 µg/ml Ascorbic acid and 5 mM β-Glycerophosphate. Similarly, GW4869 14 µM concentration treatment was repeated against vehicle group for 8 days to recapitulate the comparative inhibition in mineralization in both groups. Culture media was changed every 48 hours.

3.2. Calcein-DAPI staining for in-vitro mineralized cell culture

Cells after culturing for mineralization assay, were fixed in 10% formalin–PBS buffer and stained with 0.25% calcein solution. After fixation, the cells were washed with calcein buffer (0.15 M NaCl–2% NaHCO3). Images were captured by an EVOS FL cell imaging system at a 40 magnification (Life Technologies).

3.3. Designing guide RNA (gRNA) oligonucleotide for CRISPR construct

E-crisp.org was used and fed in the open reading frame sequences into the FASTA sequence placing '>' at the start of sequence entry. Further, select the species 'mouse' and enter gene name as *Smpd3;* then press design gRNA sequence. From the list of gRNA sequences, 'GAGGAGGCAGACATTGGCCG' is chosen following the criteria of selection- 1) Protospacer adjacent motif /NGG sequence must be adjacent to 3-prime end, 2) Sequence should match within the exon, 3) should be near ATG (start codon) or in the open reading frame and was verified by aligning with *Smpd3* sequence using the Strider software (version 3.5 z1). To clone into gRNA scaffold, two forms of oligo

5'CACCGGAGGAGGCAGACATTGGCCG 3',

5`AAACCGGCCAATGTCTGCCTCCTCC 3' are ordered (Sigma), then synthesized by forward and reverse Oligo annealing. This pair of oligos are ligated within the plasmid-pSpCas9(BB)-2A-Puro (PX459) V2.0 9175 bps purchased from Zhang lab, was digested by BbS1 restriction enzyme prior to vector: insert ligation.

3.4. Cloning and Transformation

Vector: insert (ligated material) is further transformed using competent cells (CC) bought from NEB). After combining ligated material with CC in an Eppendorf, then incubated on ice basket for 30 minutes and heat shock given to both tubes at 42 °C for one minute 30 seconds. Incubated again on ice for 2 minutes and mixed with Lysogeny broth [Multiwell, Wisent Inc.] (LB) media attached to a rotor in the incubator at 37 °C for 30 minutes and centrifuge at 10K rpm for 1 minute. Supernatant is removed and pellet in resuspended in 200 µl LB media. Borosil glass beads are used to spread bacterial suspension on LB agar with ampicillin (Amp) [100 µg/ml] plate. Final incubation for overnight until 14-16 hours is done at 37 °C. Followed by round and

isolated colonies seen on the LB agar plate are selected for inoculation, which is incubated in a shaker at 37 ℃ for overnight 14-16 hours.

3.5. Generation of Smpd3 knockout plasmid

Inoculated culture is purified using the Midi-prep kit (protocol followed as provided in the kit) from Qiagen, measured the concentration of purified plasmid DNA construct using spectrophotometry (Genesys, Thermo scientific). To analyze and confirm the vector sequence (PX-459 with insert), plasmid DNA was sent for sequencing (Nanuq services, Genome Quebec) to prime against forward primer 5`GACTATCATATGCTTACCGTA 3`.

3.6. Transfection

Post confirmation of the plasmid construct (PX-459 with insert/gRNA), to study the inactivated transcriptional regulation of *Smpd3* gene, we transfected MLO-A5 cells with *Smpd3* KO expression vector to knockout the cell group while for WT group of MLO-A5 cells, a vector (PX-459) without insert is used for transfection; for both groups by Lipofectamine 3000 transfection kit (Invitrogen) according to the supplier's instructions.

3.7. Puromycin selection

Study groups of transfected MLO-A5 cells are counted and plated on low density, such as 500 cells/µl are grown on a 10 cm tissue culture dish (Corning Incorporated, USA) and treated with Puromycin (1µg/ml) for 3 days consecutively. Culture media was changed every 48 hours. *Smpd3* knockout cells were selected in the presence of puromycin until the non-transfected control cells were dead.

3.8. Single cell clone culture

Single cell clones were picked and seeded on 24-well plate, when confluent these were expanded on 12-well plate in duplicates for each clone. Once confluent these were treated again with Puromycin (1µg/ml) to ensure the condition that clones were free of non-transfected cells, then a cryovial for each clone was frozen at –80°C and later transferred to liquid nitrogen for cryopreservation. Nine independent clones have been generated for *Smpd3* KO MLOA5 cells. Wherein duplicate sets of the same clones were centrifuged and pelleted for DNA extraction. Similarly, transfected control cells were stocked and pelleted. Stored the pellets at -20°C.

3.9. Genomic DNA isolation from single-cell clones generated using Smpd3 knockout construct

Added 600 µl DNA isolation buffer and 2µl proteinase K to each tube of pellet from clones and control MLO-A5 transfected cells, then vortexed, mixed, and incubated at 55°C for overnight. Vortex again, mix and treated with 600 µl phenol: chloroform and centrifuged for 5 minutes. Collected 500 µl upper phase from centrifuged samples and transferred it to newly labelled tubes. Added 500 µl chloroform and centrifuged for 5 minutes. Then collected 400 µl upper phase and transferred to another set of new labelled tubes. Precipitated the DNA by adding 800 µl of 100% ethanol to each tube and centrifuge for 10 minutes. Further discarded the supernatant and washed with 450 µl of 70% ethanol by sinning for 5 minutes. Discarded the supernatant and dry spin for 2 minutes. After air drying the tubes added 100 µl of 10 mM Tris to dissolve the pellet.

3.10. Q5 PCR to target altered sequence

Flanking Forward and Reverse primers were designed to target upstream and downstream of gRNA bound region in exon 2 of Smpd3 gene that produced amplicon size of around 535 base pairs in length. 5’ GTCTACCTGGCTCTGCTTGTG 3’ and 5’CGCACAATGCAGCTGTCCTCA 3’ (Sigma) used for high fidelity Q5 PCR (Q5 reagents from New England Biolabs), with annealing temperature at 61°C. PCR products were purified by using QIAquick Gel Extraction Kit Protocol and sent for sanger sequencing (Nanuq services, Genome Quebec).

3.11. Sub-cloning of single cell clone fragments

Each clone has two alleles of *Smpd3 gene* and to ensure if both alleles have been altered, segregation of PCR amplicons is required. Purified PCR products of individual clones were subcloned into pMiniT^{TM} 2.0 vector by following the NEB PCR cloning kit protocol for the quick ligation of vector: insert.

3.12. Transformation for subcloning

Ligated material is transformed using competent cells (CC) bought from NEB). Incubated on ice for 30 minutes and heat shock given for one minute 30 seconds at 42°C. Incubated again on ice for 2 minutes. Further, 750 µl LB media is added and incubated on rotating rotor for 45 minutes at 37°C. Then, 10µl of transformed mix is taken in a new eppendorf + 140 µl LB is added to dilute it and spread on LB agar with ampicillin (Amp) [100 µg/ml] plate. Incubated at 37°C for overnight.

3.13. DNA purification and sequencing

DNA fragments are purified by Purelink HiPure miniprep kit (Invitrogen, Carlsbad, USA) following the kit protocol. Sanger sequencing was done at Genome Quebec using the Nanuq platform and sequences were analyzed by the DNA Strider software.

3.14. Gene Expression analysis for Smpd3 KO MLO-A5 clone

Mineralized cell layers were lysed in 0.5 ml Trizol reagent (Ambion, Life Technologies), then total RNA was extracted and 8µg of RNA concentration is used for DNase treatment. 10 µl of DNase treated samples are used for reverse transcription. cDNA sample quality is confirmed with HPRT PCR. Further m-RNA expression of *Smpd3* is analyzed using qRT-PCR. Raw relative quantitation data is recorded for the same and statistically represented using GraphPad prism software.

3.15. Mineral deposition analysis

Control and PX-459 vector with *Smpd3* specific gRNA insert for knockout expression of SMPD3 used for transfecting MLO-A5 cells were cultured in 500mM β-Glycerophosphate and 100 µg/ml Ascorbic acid supplemented medium for 10 days. Cells were then fixed in 10% buffered formalin (Fisher Scientific), washed in PBS (2x) and stained with 0.25% calcein solution. After staining, cells were washed with calcein buffer (0.15 M NaCl–2% NaHCO3) and counter-stained with DAPI. Images were captured by the EVOS FL (Life Technologies) cell imaging system at 20X magnification.

3.16. Scanning electron microscopy (SEM) and energy-dispersive X-ray spectroscopy (EDS) characterization of MLO-A5 cells

Mineralized cell layers on 0.1% gelatin coated coverslips were fixed in 2.5% glutaraldehyde for 1 hour at room temperature. Cell layers were washed gently using 0.1 M sodium cacodylate buffer and dehydrated using ethanol gradation (30%, 50%, 70%, 80%, 90%, and 100%; for 10 min in each solution). The coverslips having the cells were then dried using critical point drying (CPD; Leica Microsystems EN COD 030 Critical Point Dryer). The dried samples were mounted on SEM aluminum stubs using adhesive carbon tape, and sputter-coated with about 20 nm platinum using an EMS 150R ES platinum sputter coater (EMS). The samples were imaged under SEM using a field emission Quanta 450 Environmental SEM (FE-ESEM) at 10 keV operating voltage under a high vacuum (FEI). EDS spectra were obtained at 15 kV in the regions of interest using an Octane Super 60 mm (Sage et al., 2010) EDS system (EDAX Inc.).

CHAPTER 4: RESULTS

4.1. Developed SMPD3 inhibitor MLO-A5 model using pharmacological agent-GW4869

SMPD3 is known to mineralize osteoblasts in bone. To examine mineralization, we generated an SMPD3 inhibitor-induced in-vitro pre-osteocytic model using GW4869, an inhibitor of SMPD3. In a concentration-dependent study, MLOA5 cells were treated for 6 days with 12, 13 or 14uM SMPD3 inhibitor and compared to a vehicle control. Calcein-DAPI stained matrix minerals showed a concentration-dependent negative correlation with the highest inhibition efficiency using the 14uM GW4869 concentration. The control vehicle showed denser mineral deposition as compared to the inhibitor-treated samples (Fig. 4A). The 14uM concentration after 8 days of treatment exhibited sparse mineral deposition as compared to the vehicle control (Fig. 4B). Examining cells using scanning electron microscopy comparing the vehicle control to the cells treated for 10 days with 14uM GW4869 treatment showed fewer mineral deposits in the latter compared to the former.

4.2. Generation of SMPD3 knockout model using CRISPR-CAS-9 vector

Using the Strider software, a guide RNA (gRNA) oligo sequence was designed and aligned to the mouse *Smpd3* gene target sequence within the exon-2 of the gene (Fig. 5A) and was precisely designed to ligate within the vector sequence. The vector is made up of several components including a U6 promoter, a Cytomegalovirus (CMV) enhancer**,** a chicken β-actin (CBA) promoter, an intron, 2 nuclear localization signal **(**NLS) and two genes CAS9 and $Puro^R$. The gRNA sequence is transcribed and expressed by a U6 and chicken β-actin (CBA) promoters and a Cytomegalovirus (CMV) enhancer. U6 initiates the process and is aided by the CMV enhancer and CBA promoter. The vector, using the CRISPR mechanism, will be cut using the restriction enzyme, BbSI at the restriction site. (Fig.5B). The SV 40 NLS helps the entry of the CAS-9 gene into the nucleus and the nucleoplasmin NLS for its exit. The $Puro^R$, Puromycin resistance gene, helps in cell selection. The vector has been digested with the

restriction enzyme BbS1 at two sites, producing staggered ends (Fig.5C). Furthermore, ligase was used to allow the insertion of the double stranded oligonucleotide (gRNA) into the plasmid (Fig5D).

4.3. Generation and screening of a *Smpd3* knockout model using CRISPR approach

SMPD3 enzyme production could be reduced or not produced when *Smpd3 is* knocked out in the pre-osteoblastic MC3T3 and pre-osteocytic MLO-A5 cell-lines. This knockout model, which is deficient in SMPD3, will be useful to examine its deficiency on mineralization. Once the gRNA is ligated within the CRISPR-CAS-9 vector, transfection *in vitro* leads to the incorporation of the plasmid into the nuclei of MC3T3 and MLO-A5 cells resulting in the interruption of the *Smpd3* site that codes for the SMPD3 enzyme. Transfected cells are cultured and Puromycin, an antibiotic, added. Since the plasmid has a Puromycin resistant gene, cells that do not incorporate the plasmid will die and only transfected cells having the plasmid will be selected. After the selection is complete, 10-15 single cell colonies are picked from the cell cultures and cultured in duplicates for future use and DNA isolation (Fig 6). Extracted DNA from these clones are then amplified by PCR (Fig.7A, B), using forward and reverse primers targeting the region surrounding the protospacer adjacent motif (Fig. 7A, in red) where the alteration may have occurred. To confirm if there are changes in the nucleotide sequence as expected including insertions or deletions, the PCR amplification product is purified and sent for DNA sequencing (Fig. 6, 7C). The probable clone and WT sequence chromatograms, generated from DNA sequencing, are compared for differences in their peaks, representing the sequence of nucleotides (Fig.7C).

4.4. Development and detection strategy for clones with homozygotic mutations

Every gene has two copies known as alleles that may or may not differ from each other. Similar alleles exhibit a homozygous expression, while different alleles show a heterozygous expression. Therefore, it is essential to identify the potential clones that exhibit homozygotic mutations to develop a knockout model. To achieve this effect, a PCR is performed using DNA isolated from single-cell clones. The resulting PCR-amplified product is then purified and used for subcloning; a technique used to separate the alleles. Following this separation, each fragment is ligated within a pMini T 2.0 vector which is later transformed. Inoculation is then performed to increase the plasmid yield. Thereafter, the plasmids are purified by Mini preparation followed by DNA sequencing (Fig.8).

4.5. Chromatograms for DNA sequenced subcloned fragments of potential Knockout clones

Initially, sequenced DNA is analyzed using chromatograms. These chromatograms will detect sequence alterations in DNA fragments by comparing fragment peaks to those of WT peaks. These alterations could reflect a heterozygous, homozygous, or mixed clone traits. We are very much interested in obtaining a homozygous trait as it would reflect a *smpd3* gene knockout model. Initially, we saw three altered fragment peaks compared to WT showing the presence of a third allele (Fig.9A), reflecting the possibility of having a mixed clone. Since this may not be homozygous, this clone was excluded from our studies. For the next clone (Fig.9B), only one sequence alteration was observed while the other sequenced fragment matched the WT sequence peaks, clearly pointing to a heterozygous clone. For another sequenced clone (Fig.10), the change in fragment peaks, as compared to WT sequence, were noticed right after the PAM sequence (TGG) for the first sequenced fragment, while PAM was lost in the second

sequenced fragment. From this data, it is clear that this clone (Fig.10) is potentially *Smpd3* gene knocked out for both allelic copies and is essentially homozygous.

4.6. Comparison of open reading frame (ORF) patterns and protein alignment of subcloned fragments as compared to control (WT) after sequencing of probable *Smpd3* knockout clones.

In an open reading frame, the nucleotide codes are transcribed into amino acid codes for proteins. By analyzing the protein translated sequences, it is possible to infer the difference of proteins produced by the WT clone and that of a potential knockout clone. In the first clone (Fig.11A) pattern I, the WT protein sequence is aligned well with that of the clone fragment before and after the interruption. Since the frame is restored afterwards, this indicates that the protein might still be produced. However, patterns II and III did match initially but interruptions were noted later. (Fig.11A). Since the protein could also be generated in this case, this clone is not useful. This is in concordance with the earlier result noted (Fig. 9A). For the subsequent clone's protein translation analysis (Fig.12A) pattern I matched the WT sequence as expected and noted earlier (Fig.9B). On the other hand, pattern II did not match, confirming a heterozygous clone. In the next clone's protein analysis (Fig.13A), Both patterns I and II did not align with WT protein sequence. This implied that neither the clone's gene sequence (Fig.10A) nor the open reading frame (Fig.13A) matched that of WT indicating that the clone could be considered as a useful *Smpd3* knockout model.

4.7. Characterization of *Smpd3* knockout Clone 2 model

SMPD3 expression at mRNA level was analyzed as higher for WT cells (vector control without insert) than the *Smpd3* Knockout MLO-A5 cells, which was notable here (Fig.14A). This was

done for day 0 culture of cell groups when it is expected to show the SMPD3 activity right before being differentiated from late-stage osteoblasts to osteocytes. In the in-vitro mineralization assay, differences in deposition of minerals were noted between Control WT and knockout clone 2 model MLO-A5 cells. Calcein-Dapi stained images show decreased mineral density knock-out model compared to WT. This difference confirms the lack of mineral deposition in SMPD3 enzyme deficient cells (Fig.15A). MLO-A5 cell layers were further characterized using scanning electron microscopy (SEM) to confirm the localization of mineral deposits (Fig.16). SEM images showed crystalline hydroxyapatites present in control group (Fig. 16 A), but in knockout group with fewer minerals confirmed by the elemental analysis by EDS showed only tiny amounts of calcium (Ca) and phosphorus (P) in some spots on these samples (Fig. 16 B). EDS showed that minerals were deposited on the cells with high Ca and P atomic percentages (Fig. 16A), while it was lower in knockout groups (Fig.16 B).

4.8. Figures (see below):

Figure 4

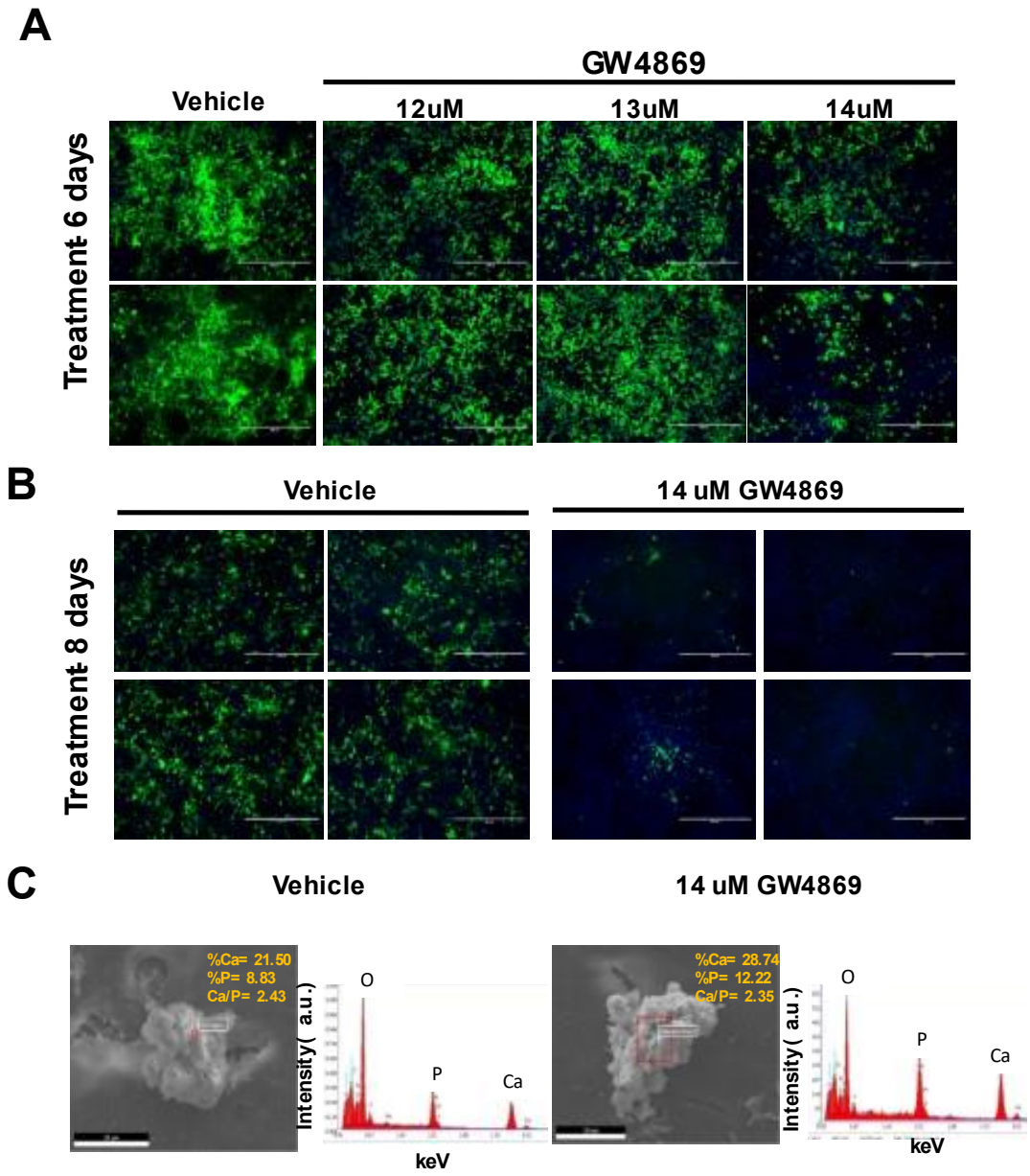

Figure 4: Established SMPD3 inhibition in *in vitro* osteoblastic model using GW4869. A. Dose-dependent SMPD3 Inhibitor treatment, at 12uM, 13uM and 14uM concentrations of MLOA5 cells against vehicle control at 6 days and stained with Calcein-DAPI. **B.** A concentration 14uM SMPD3 for 8 days as compared to vehicle control showed increased deposition of minerals in the control specimen **C.** SEM-EDX analysis for vehicle vs. GW4869 treated group showing Ca/P ratio and % weight by spotting. This characterizes the nature of mineral phases of both the groups.

Figure 5

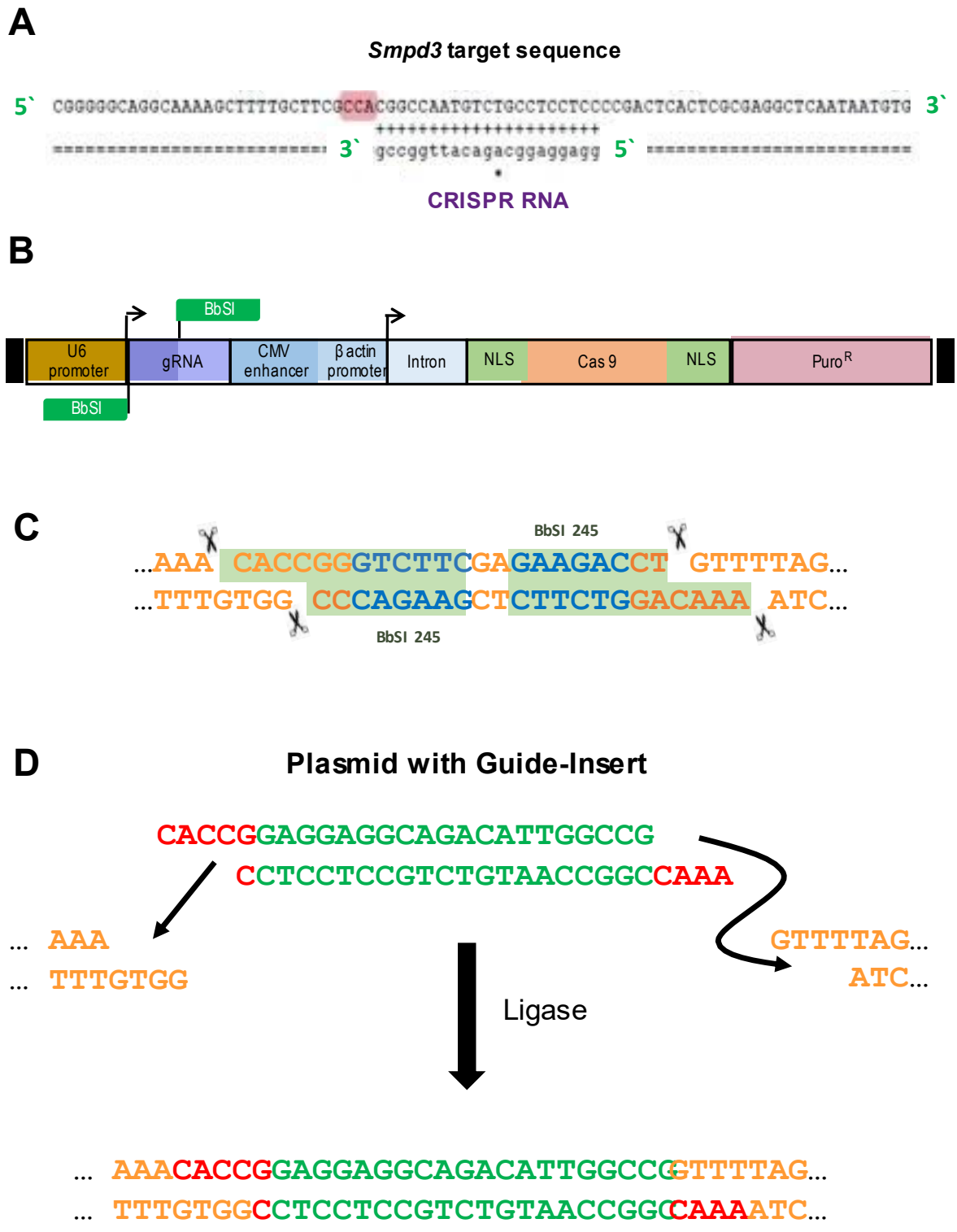
A
Smpd3 target sequence
5` CGGGGGCAGGCAAAAGCTTTTGCTTCGCCACGGCCAATGTCTGCCTCCTCCCCGACTCACTCGCGAGGCTCAATAATGTG 3`
3` gccggttacagacggaggagg 5`
CRISPR RNA
B
BbSI
U6 promoter
gRNA
CMV enhancer
β actin promoter
Intron
NLS
Cas 9
NLS
Puro^R
BbSI
C
BbSI 245
...AAA CACCGGGTCTTCGAGAAGACCT GTTTTAG...
...TTTGTGG CCCAGAAGCTCTTCTGGACAAA ATC...
BbSI 245
D
Plasmid with Guide-Insert
CACCGGAGGAGGCAGACATTGGCCG
CCTCCTCCGTCTGTAACCGGCCAAA
... AAA
... TTTGTGG
GTTTTAG...
ATC...
Ligase
... AAACACCGGAGGAGGCAGACATTGGCCGGTTTTAG...
... TTTGTGGCCTCCTCCGTCTGTAACCGGCCAAAATC...

Figure 5: Generation of *Smpd3* knockout model using CRISPR method.

A. Alignment of Oligo sequence with *Smpd3* cDNA sequence using the Strider software **B.** Schematic vector map including CRISPR mechanism components showiing sites of the restriction enzyme. Components include: U6 promoter, which transcribes the expression of gRNA together with Cytomegalovirus (CMV) promoter and chicken β-actin promoter, followed by a hybrid intron sequence, SV40 nuclear localization signal (NLS) for the entry of CAS9 gene into the nucleus of a eukaryotic cell and a nucleoplasmin NLS for its exit; $Puro^R$- Puromycin resistance gene for cell selection. **C.** A diagram showing the positions of nucleotides in the vector at two restriction sites-staggered ends cut by the BbSI enzyme. **D.** A schematic diagram showing the ligated mouse *smpd3* gene- specific gRNA in the vector.

Figure 6

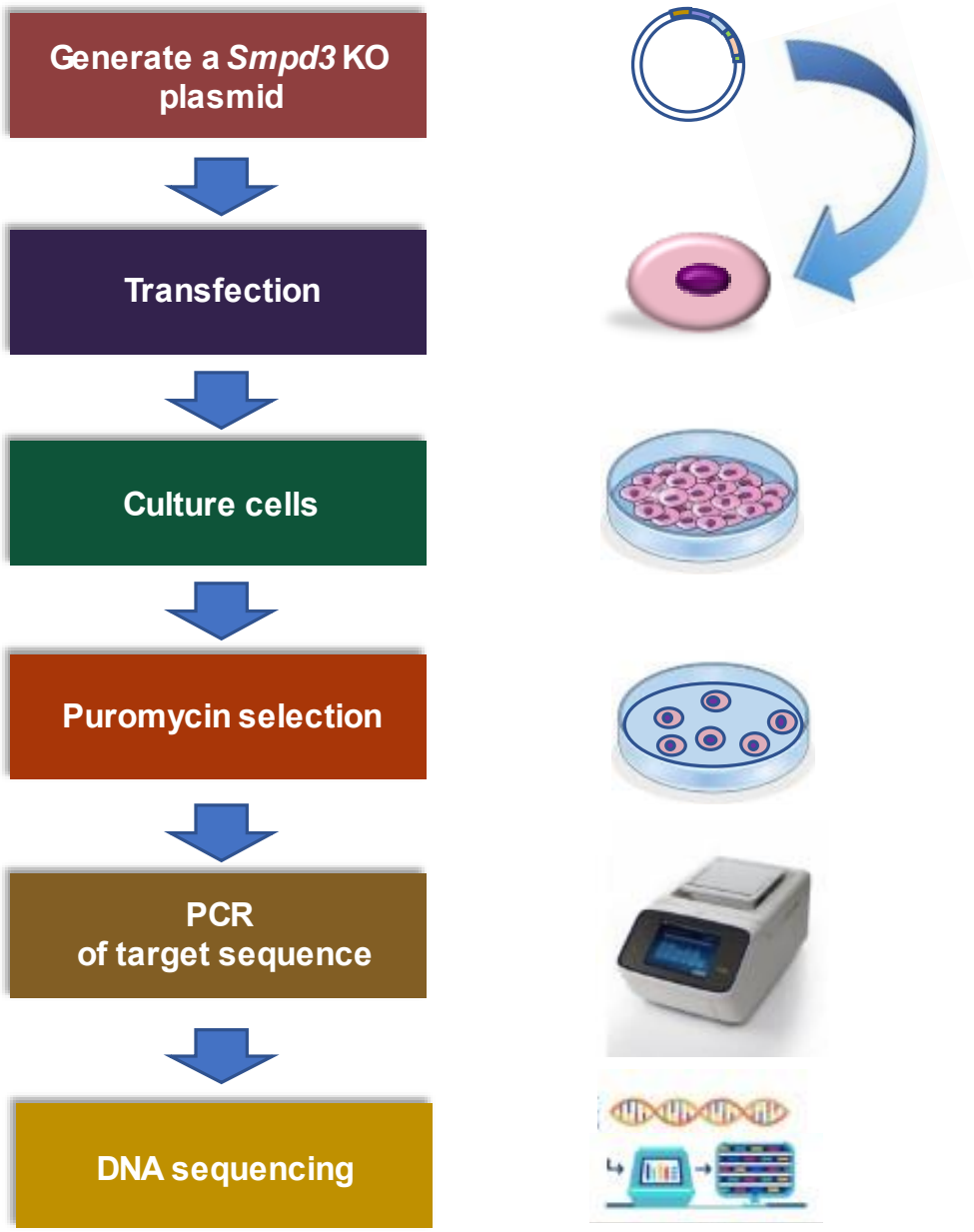

Figure 6: Generation and screening of a *Smpd3* knockout model using CRISPR approach. Technical steps of the procedures leading to the generation of the knockout *in vitro* model.

Figure 7

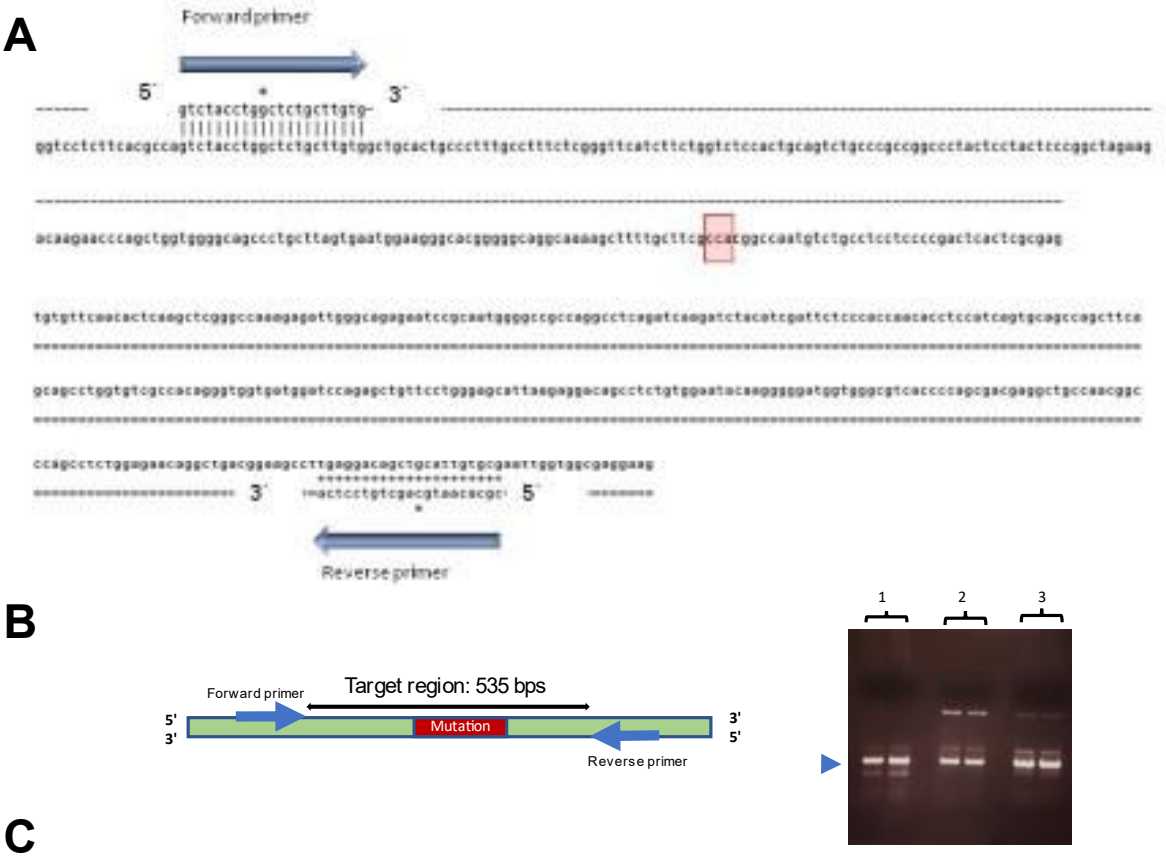

Figure 7: Generation of *Smpd3* knockout model using CRISPR method. A. Strider view of the forward and reverse primers aligned to *Smpd3* gene sequence. B. Graphical representation of target region PCR and its product showing the band size. C. DNA-sequenced chromatogram of WT MLO-A5 clone vector control without insert and probable *Smpd3* knockout clone.

Figure 8

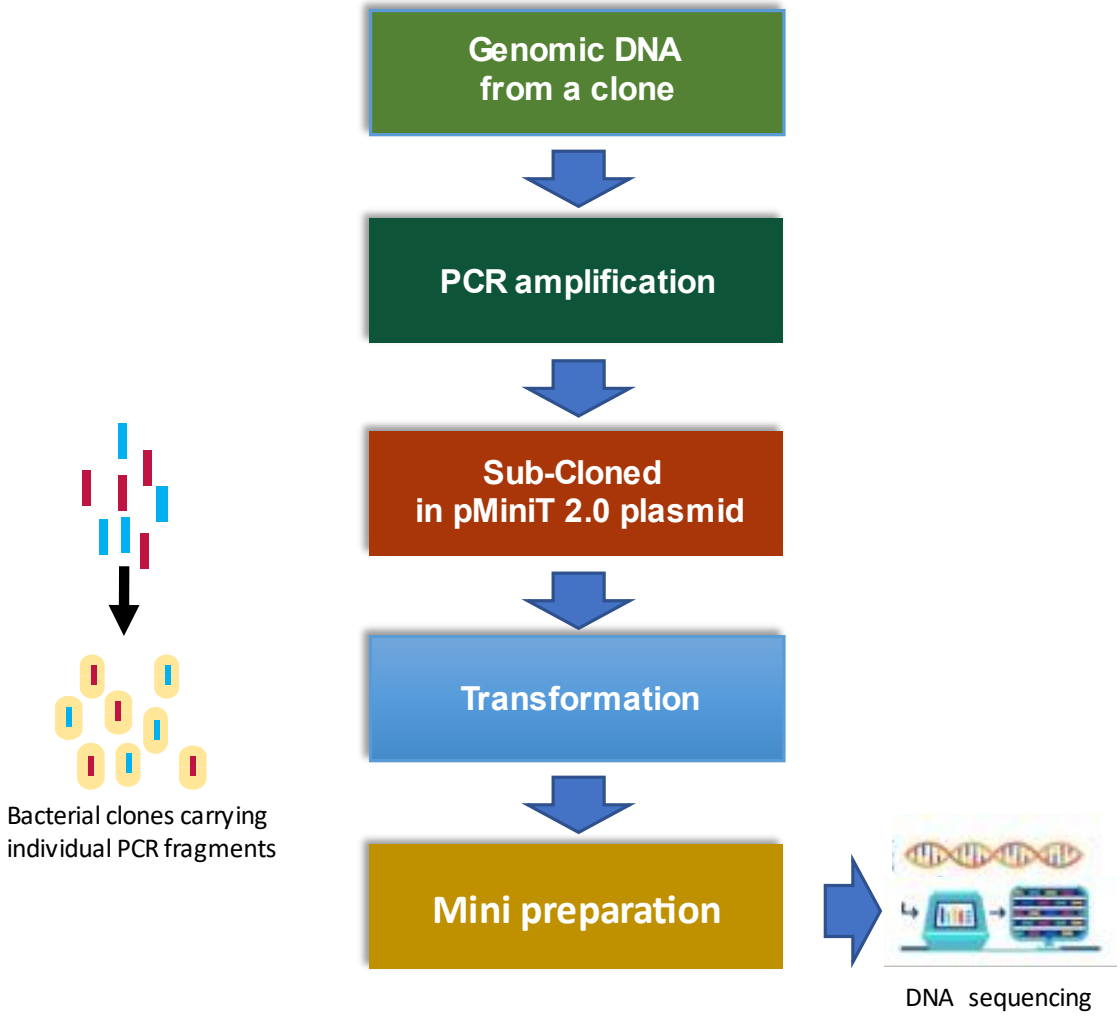

Figure 8: Development and detection strategy for clones with homozygotic mutations. Flowchart of strategies used to confirm the possibility of a *Smpd3* knockout model by segregation of alleles using DNA sequencing for subcloned samples.

Figure 9

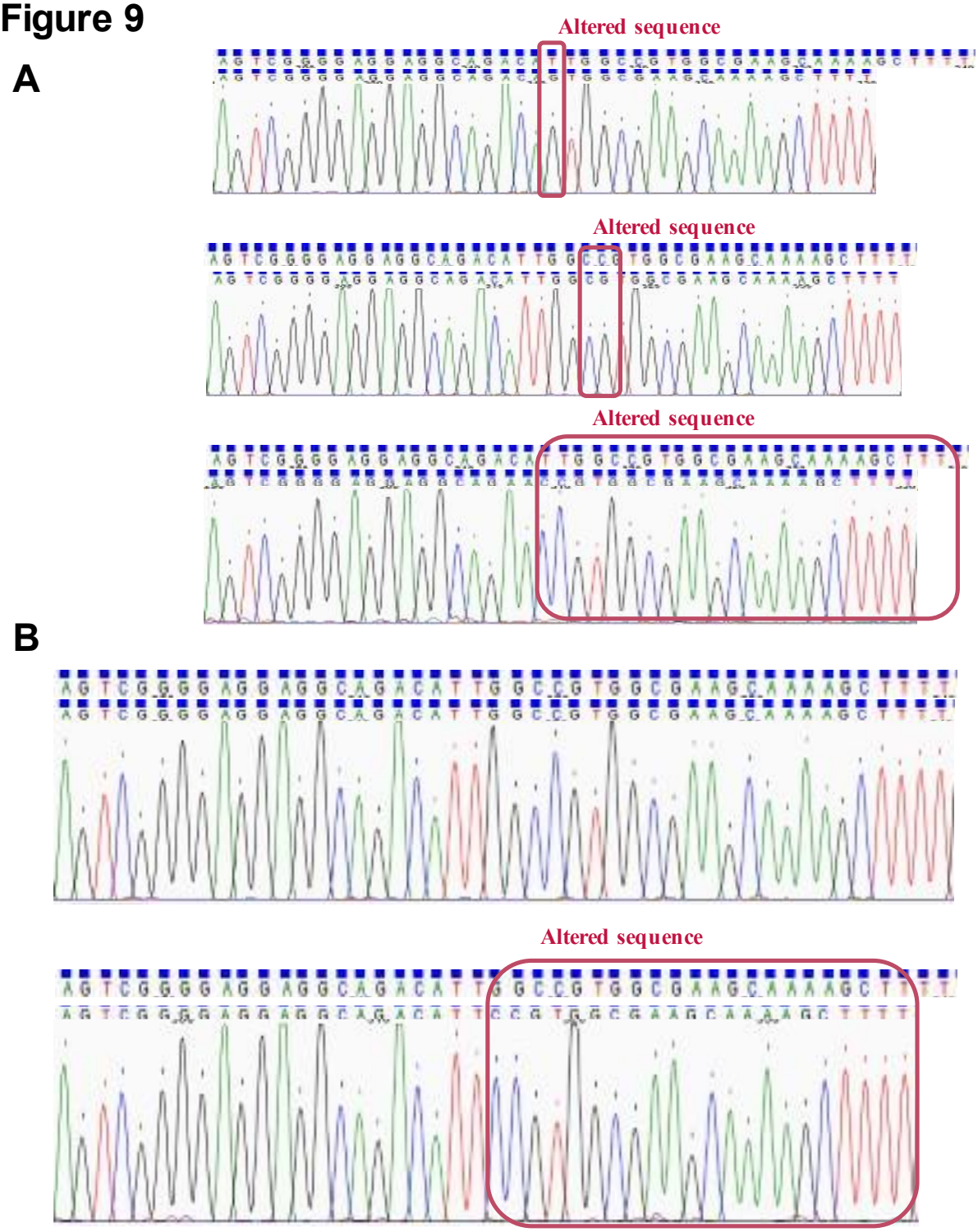

Figure 9: Chromatogram for DNA sequenced subcloned fragments of probable Knockout subcloned fragments. Representative clones carrying a mixed allelic and single allelic mutations. A. Clone 1: Three chromatogram patterns of altered nucleotide sequences were observed, when peaks were compared with WT sequence (the first line of each). Since three different fragments are sequenced in this clone, that could indicate a mixed clone. **B.** Clone 1.1: the first chromatogram peaks matched with the WT one, whereas the second chromatogram showed difference in peaks indicating a single allelic mutation which could be considered as a heterozygous clone.

Figure 10

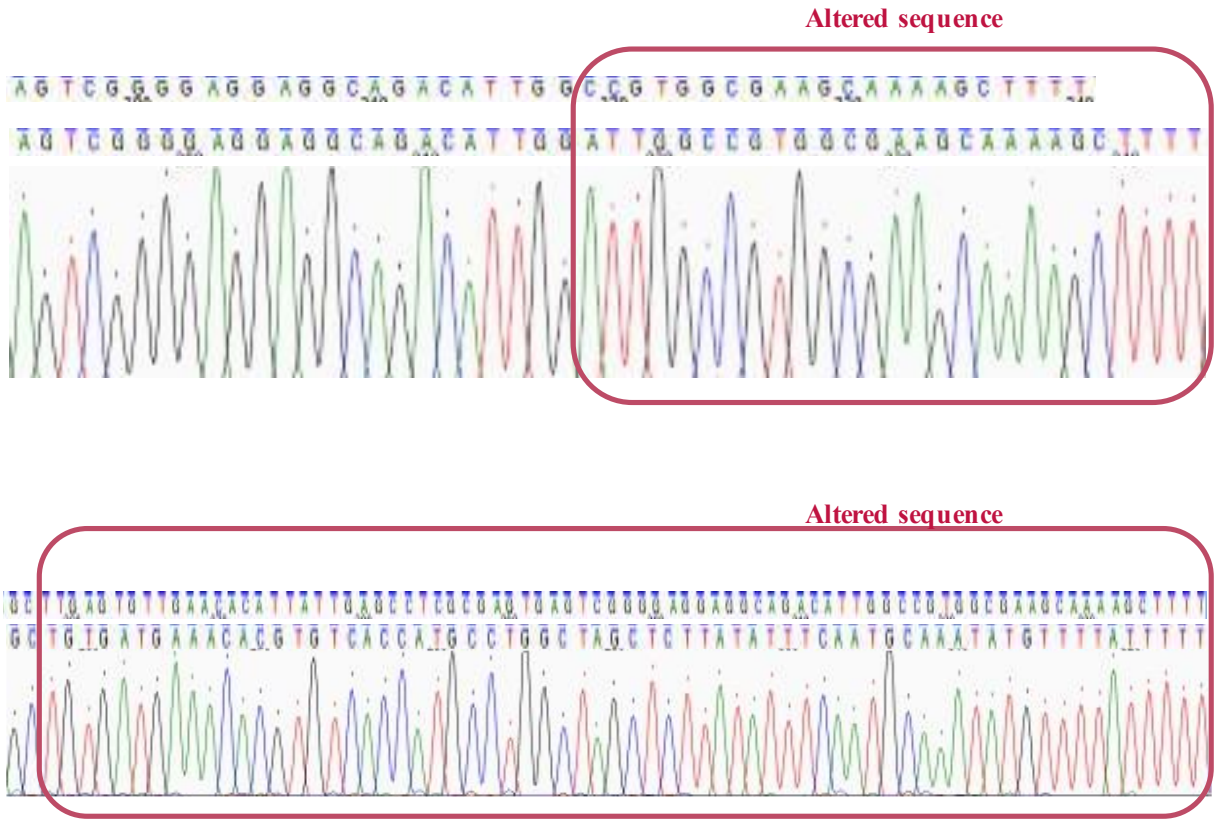

Figure 10: Chromatogram for DNA sequenced subcloned fragments of probable Knockout subcloned fragments. A. Both chromatograms showed difference in peaks compared to WT indicatinga double allelic mutation which could be considered as a homozygous clone.

Figure 11

A

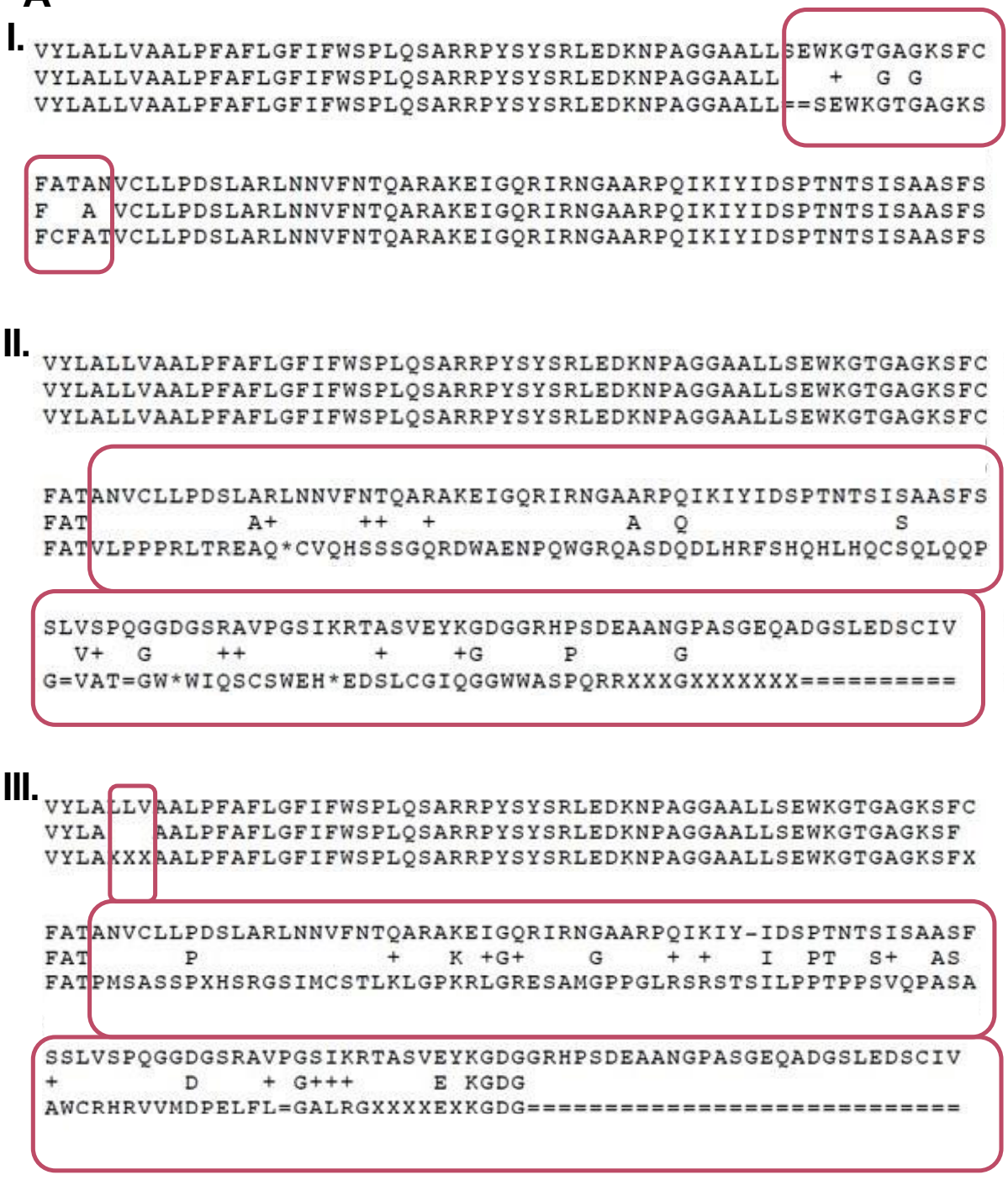

Figure 11: Comparison of open-reading frames (ORF) patterns and protein alignment of *Smpd3* probable knockout clone subcloned fragments to control (WT). Clone 1. A. Pattern I shows a transient interruption of the ORF, of the subcloned fragment as compared to WT, which was restored. This implies that the protein is produced aa in WT. Patterns II and III showed a continuous interruption of the protein coding sequence indicating that the protein production is altered. Magenta highlights indicate alterations in ORF.

Figure 12

A

I.

```
VYLALLVAALPFAFLGFIFWSPLQSARRPYSYSRLEDKNPAGGAALLSEWKGTGAGKSFC
VYLALLVAALPFAFLGFIFWSPLQSARRPYSYSRLEDKNPAGGAALLSEWKGTGAGKSFC
VYLALLVAALPFAFLGFIFWSPLQSARRPYSYSRLEDKNPAGGAALLSEWKGTGAGKSFC

FATANVCLLPDSLARLNNVFNTQARAKEIGQRIRNGAARPQIKIYIDSPTNTSISAASFS
FATANVCLLPDSLARLNNVFNTQARAKEIGQRIRNGAARPQIKIYIDSPTNTSISAASFS
FATANVCLLPDSLARLNNVFNTQARAKEIGQRIRNGAARPQIKIYIDSPTNTSISAASFS

SLVSPQGGDGSRAVPGSIKRTASVEYKGDGGXTPATRL--------------------
SLVSPQGGDGSRAVPGSIKRTASVEYKGDGG  P+
SLVSPQGGDGSRAVPGSIKRTASVEYKGDGGRHPSDEAANGPASGEQADGSLEDSCIV
```

II.

```
VYLALLVAALPFAFLGFIFWSPLQSARRPYSYSRLEDKNPAGGAALLSEWKGTGAGKSFC
VYLALLVAALPFAFLGFIFWSPLQSARRPYSYSRLEDKNPAGGAALLSEWKGTGAGKSFC
VYLALLVAALPFAFLGFIFWSPLQSARRPYSYSRLEDKNPAGGAALLSEWKGTGAGKSFC

FATANVCLLPDSLARLNNVFNTQARAKEIGQRIRNGAARPQIKIYIDSPTNTSISAASFS
FAT  +     +      V ++ +  ++  +  + G  R Q     D    +       S
FATECLPPPRLTREAO*CVOHSSSGORDWAENPOWG==R=OASDO=DLHRFSHOHLHOCS

SLVSPQGGDGSRAVPGSIKRTASVEYKGDGGRHPSDEAANGPASGEQADGSLEDSCIV
 L  P    G   +              G  G   +     G
QLQQPGVATGW*WIQSCSWEH*EDSLCGIQGGWWASPQRRG=================
```

Figure 12: Comparison of open-reading frames (ORF) patterns and protein alignment of Smpd3 probable knockout clone subcloned fragments to control (WT). Clone 1.1 A. A. Pattern I shows no interruption of the ORF, of the subcloned fragment as compared to WT. Pattern II indicates that the protein production was altered. Magenta highlights indicate alterations in ORF.

Figure 13

A

I.

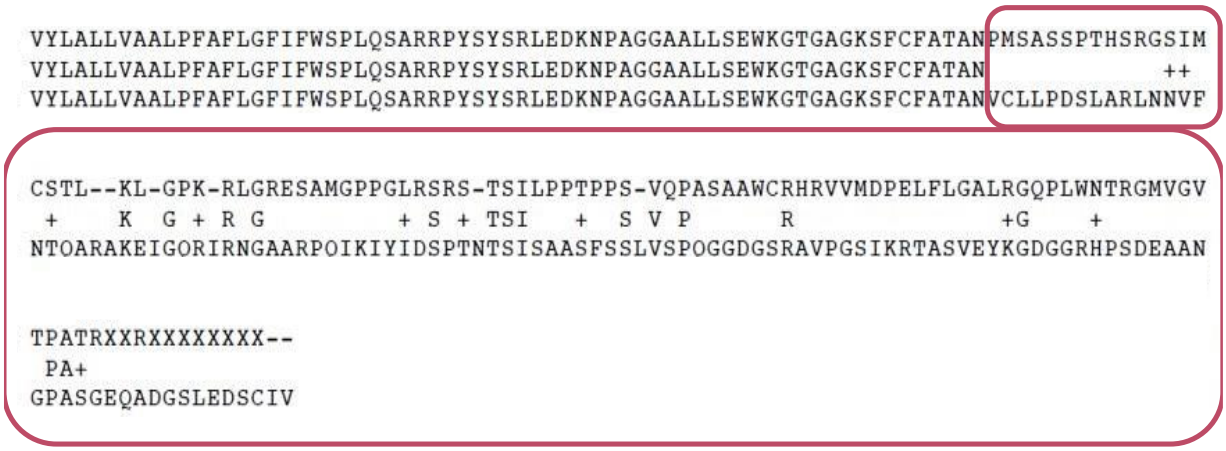

II.

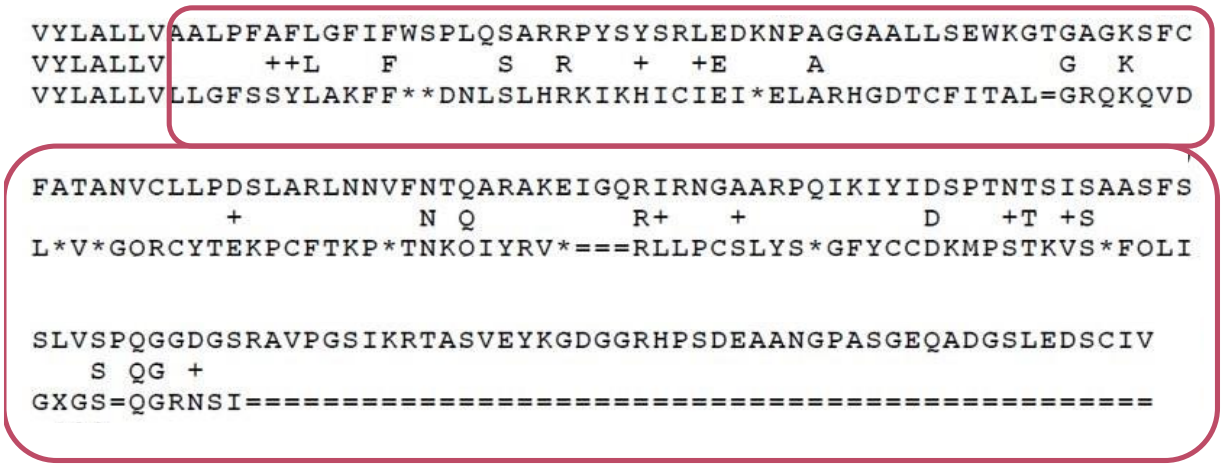

Figure 13: Comparison of open-reading frames (ORF) patterns and protein alignment of Smpd3 probable knockout clone subcloned fragments to control (WT). Clone 2 A. Patterns I and II showed that there is amino-acid interruption in the protein coding sequences confirming the presence of mutated alleles. The protein production is altered. Magenta highlights indicate alterations in ORF.

Table 1.

Clone ID	No. of subcloned amplicons sequenced	WT sequence frequency	Mutated sequence frequency	Types of mutated sequences
MLOA5 (1)	8	0	8	3
MLOA5 (1.1)	3	1	1	1
MLOA5 (2)	6	0	2	2

Table 1. Record of the number of times subcloned and sequenced for each clone and their corresponding allelic expression. MLO-A5 Clone 1- mixed clone. MLO-A5 Clone 1.1- heterozygote clone. MLO-A5 Clone2-Sequenced for 6 six times and obtained these patterns repeatedly which indicates this is a *Smpd3* knockout clone (homozygotic) type.

Figure 14

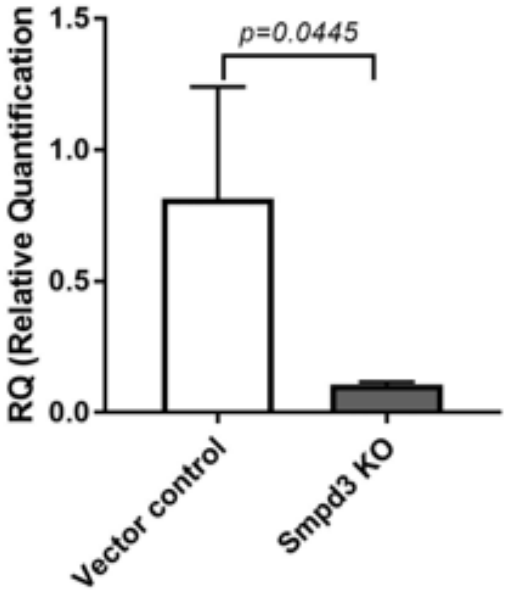

Figure 14: Characterization of *Smpd3* knockout Clone 2 qRT-PCR analysis of vector control vs. Knockout MLO-A5 clone for day 0 samples. SMPD3 expression at mRNA level is higher in WT cell than the knockout model, p value calculated by GraphPad prism software .

Figure 15

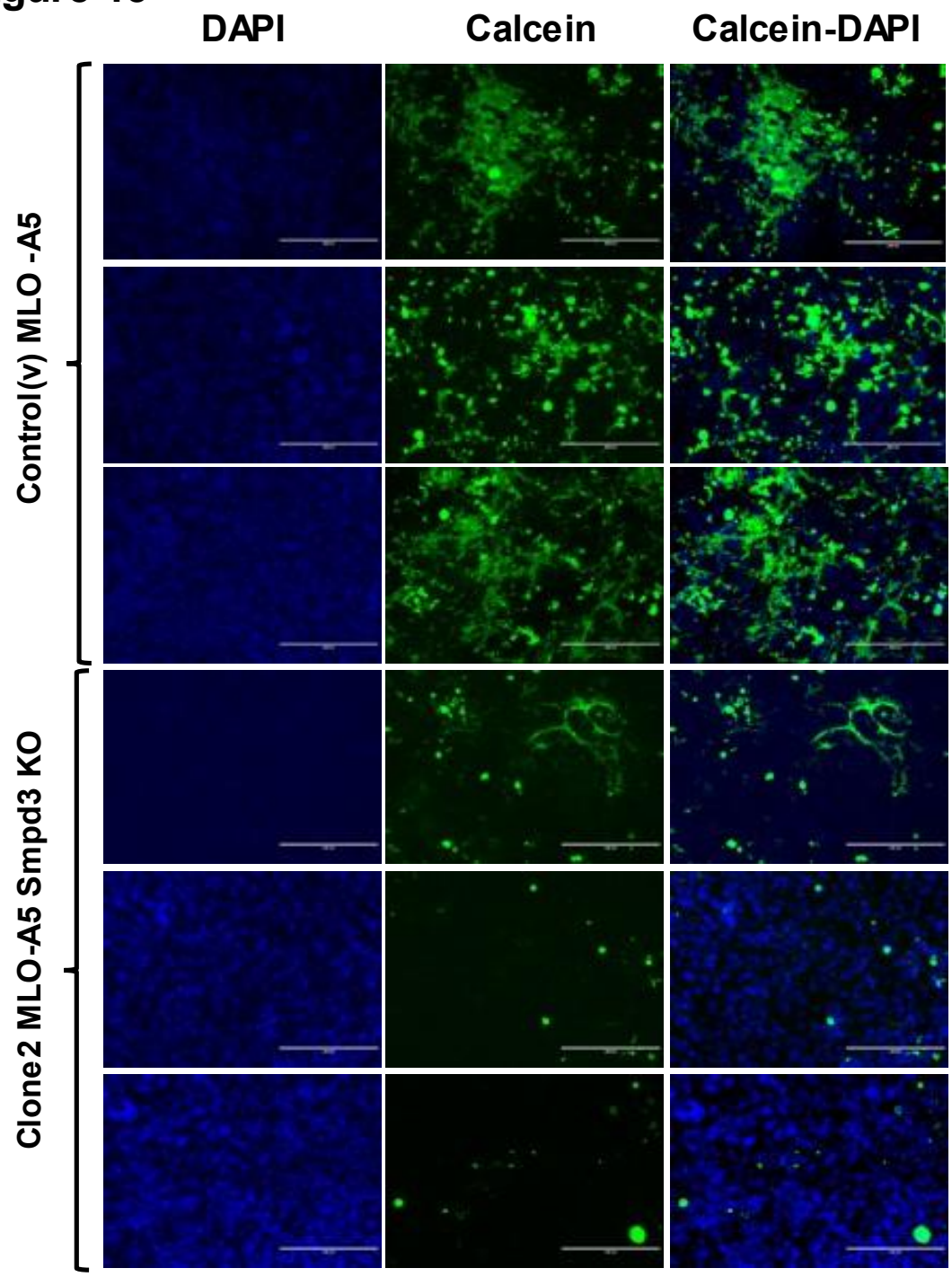

Figure 15: Characterization of *Smpd3* knockout Clone 2 A. Calcein-Dapi stained (20X) for *Smpd3 KO* clone 2 MLOA5 cell line showing reduction in mineral deposition as compared to MLOA5 vector control without insert.

Figure 16

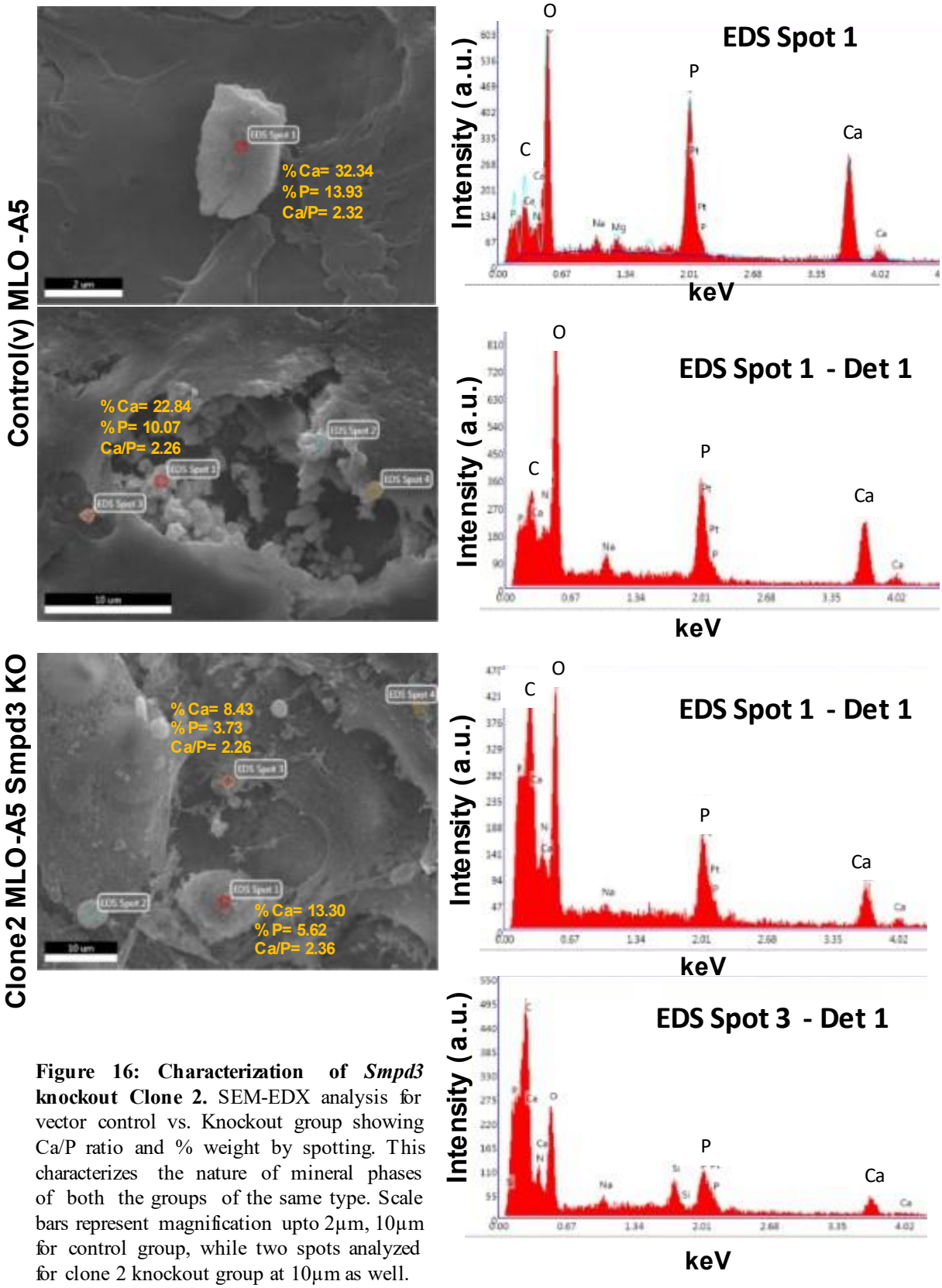

Figure 16: Characterization of *Smpd3* knockout Clone 2. SEM-EDX analysis for vector control vs. Knockout group showing Ca/P ratio and % weight by spotting. This characterizes the nature of mineral phases of both the groups of the same type. Scale bars represent magnification upto 2µm, 10µm for control group, while two spots analyzed for clone 2 knockout group at 10µm as well.

CHAPTER 5: DISCUSSION

ECM mineralization is a critical physiologic protects regulated by both local and systemic factors. This process is controlled by genetic pathways. While many of the critical determinants of ECM mineralization are well-identified, there are still some newly identified regulators/pathways for which detailed mechanistic studies are missing. One such regulator is an intracellular, cell membrane-bound enzyme SMPD3, which is essential for cartilage, bone, and tooth mineralization[66,67]. Currently, the mode of action of SMPD3 in the regulation of ECM P_i mineralization is unknown.

We propose that SMPD3 is responsible for the release of MVs, which supply a protected environment for nascent hydroxyapatite crystal formation. It is also possible that SMPD3 generates phosphoryl choline by cleaving membrane sphingomyelin, which is cleaved by another intracellular enzyme PHOSPHO1 to generate free P_i[66,67]. Within the MVs P_i can precipitate with calcium as calcium phosphate salts which later can mature into hydroxyapatite crystals[36,117]. Although this mechanism of the initiation of ECM mineralization is a likely one, we do not have enough experimental evidence that this is indeed the case. This thesis aims at generation of novel cell culture models of osteogenic cells lacking SMPD3 which will be helpful to understand the mode of SMPD3's action in the regulation of ECM mineralization.

Usefulness of cell culture models

Cell culture systems seek to recapitulate the events in the development of the tissue in-situ[92]. While some culture systems start with preformed substrates and others rely on the differentiation, proliferation, and maturation of cells, the end goal is the formation of an analogue of naturally occurring tissue [92]. Questions that arise during these studies may include whether under a given condition, the cells in question have an altered ability to form this tissue, what the role of the genetic modification might be, or whether the material formed can be used

to repair and replace native tissue [92]. To understand the cell culture method advantages, it is necessary to first review the composition of these tissues and the cells involved in their formation. In bone biology, there are multiple cell culture models well-characterized for their ability to form minerals on and within the collagen-rich ECM deposited by the cultured cells[92]. The cells are often cultured in medium containing ascorbic acid and β-glycerol phosphate (osteogenic medium) [92]. Ascorbic acid is necessary for the post-translational modifications of collagen and facilitates the triple helix formation [92,93]. Signaling through integrin receptors interacting with collagen is critical for osteogenic differentiation. On the other hand, β-glycerol phosphate acts as a substrate for tissue nonspecific alkaline phosphatase (TNAP/ALPL), a marker for functional osteoblasts[93,94,95]. ALPL activity generates free P_i, which precipitates with calcium as calcium phosphate minerals[93]. Thus, the osteogenic medium promotes osteogenic differentiation and enables the investigator to perform a functional assay for in vitro mineral deposition, indicating that the culture contains functionally active osteoblasts[92,93].

Use of MLO-A5 cells in the current project

Murine MLO-A5 cells are late osteoblastic cells which can differentiate to osteocytes[93,94,96]. The key reason we selected these cells is that they rapidly form a collagen-rich ECM, which mineralizes when cultured in an osteogenic medium having ascorbic acid and β-glycerol phosphate[97,98,99]. In our hands, these cells mineralize more consistently than MC3T3.E1 cells, the other more commonly used pre-osteoblastic cell line. As shown in the result section, the expression of SMPD3 in these cells further justifies their use in our experiments. Another reason for selecting MLO-A5 for our current study is that this is a relatively new cell line and less characterized than other well-reported cell lines. Although for the ease of manipulation

and handling, we have decided to use a cell line, any obtained data must be validated using primary cells from mice lacking SMPD3 and in vivo experiments.

Choice of approaches: Pharmacologic inhibition vs. gene 'knockout'

In the current thesis, we used both pharmacologic as well as a gene 'knockout' approach using the CRISPR/Cas9 method. SMPD3 activity has been shown to be inactivated by a chemical inhibitor GW4869, which is the most widely used pharmacological agent for blocking exosome generation[100]. GW4869 inhibits the ceramide-mediated inward budding of multivesicular bodies (MVBs) and release of mature exosomes from MVBs[66,100,101]. It was first used by Kosaka *et al.* to successfully inhibit exosome release in HEK.293 cells[102]. Studies determined pro-inflammatory effects of exosomes derived from LPS-treated macrophages, and then examined the consequence of GW4869-mediated inhibition of exosomes on cytokine production in LPS-treated macrophages *in vitro*[100,101,103].

Although GW4869 may also inhibit other sphingomyelinases, the justification of its use in our study came from published works showing that except for SMPD3, other sphingomyelinases are not essential for bone mineralization in vivo. This in vivo finding suggests that even if GW4869 inhibits other sphingomyelinases in mineralizing cells, it will be the inhibition of SMPD3 only that will affect ECM mineralization. However, like any pharmacologic approach, a limitation of this method could be that there might be yet unknown off-target effects of GW4869 that can reduce mineralization. In order to rule out this possibility we also used a CRISPR/Cas9-based approach to 'knock-out' SMPD3.

Another concern of the pharmacologic approach is that the chemical used to inhibit SMPD3 and/or the solvent in which the chemical is solubilized may affect the process of the mineral maturation and property of the minerals. Some of these treatments can change the properties

of the mineral. In the field of bone mineralization study, often the analyses are focused on whether there are more or less minerals deposited after a given time, and truly little or no attention is given on what kind of mineral species are present and what are their relative abundance. Apart from routine staining methods more advanced methodologies such as X-ray diffraction, Raman spectroscopy, SEM can be used. In our case however, we observed that GW4869 treatment of MLO-A5 cells reduces the mineral amount; mineral properties do not appear to be changed as we could detect the presence of hydroxyapatite minerals in the inhibitor-treated cultures(Fig.4 B, C).

A genetic 'knockout' approach is a relatively clean method than the pharmacologic inhibition approach. With the current advancement of technologies, it is possible to target a particular gene. However, gene targeting in cells in vitro can also show some off-target effects. Unlike an in vivo system, such off-target events cannot be segregated by breeding. However, generating multiple clones with same traits is a standard procedure to rule out such possibilities. Our observation that both the pharmacologic and gene-targeting approach show similar poor mineralization traits when SMPD3 activity was inhibited or *Smpd3* gene was knocked out, respectively, validates both the approaches.

CRISPR/Cas9 approach over gene knockdown

RNAi (RNA interference) silences genes by generating knockdowns at the mRNA level, while CRISPR generates knockouts at the DNA level[81]. RNAi functionality using exogenous double stranded RNAs, RNA interference is also triggered by the endogenously present single-stranded hairpin microRNAs (miRNA) in cells, small interfering RNAs (siRNA), or short hairpin RNAs (shRNA)[81,104]. Whereas in CRISPR, high-quality synthetic guide RNA allows the delivery of CRISPR components complexed in a ribonucleoprotein (RNP) format, which

enables the highest editing efficiencies and the most reproducible CRISPR results [81]. A major difference between RNAi and CRISPR is that RNAi reduces gene expression at the mRNA level such as knockdown, while CRISPR completely and permanently silences the gene at the DNA level known as gene knockout [81,104].

Knockouts are effective in completely blocking protein expression, dropping any confounding effects from remnant low levels of protein expression post knockdown [78,81]. As CRISPR became popular for its ease of genetic editing, variations in the method and new versions of CRISPR-associated nucleases enabled researchers to use CRISPR for applications beyond gene knockouts. For instance, CRISPRi allows the silencing of genes without permanently knocking out the gene [81]. This is achieved using a dead Cas9 nuclease that physically blocks RNA polymerase and inhibits gene transcription or by editing gene regulators to modulate gene expression. Although the mechanism is different from knocking out genes, the inhibition still occurs at the DNA level [81,104]. Recently, researchers have developed nuclease variants that can target RNA instead of DNA, yielding an outcome like RNAi [81].

Main limitation of the RNAi silencing method is that it suffers from high off-target effects. Silencing unintended RNA targets results in modified phenotypes and is therefore detrimental for gene function screening experiments [81]. The off-target effects in RNAi are found to be sequence-independent and sequence-dependent. In 2003, a study showed for the first time that siRNA also targeted sequences with limited complementarity[81]. Even today, sequence-based off-target effects are still the most challenging issue in RNAi experiments. The CRISPR system initially also had some sequence-specific off-target effects, but efficient design tools aid in finding guide RNAs that show minimal off-target effects [81]. The introduction of sgRNA and further chemically modified sgRNAs have also greatly contributed to reducing the off-target effects compared to plasmid and IVT-derived guide RNAs[81]. Currently, CRISPR has appeared as a valuable tool in target identification and validation studies, particularly with the

availability of arrayed synthetic sgRNA libraries and this format supplies easy data deconvolution comparatively than pool format, since synthetic sgRNA achieves consistently high editing efficiencies [78,81].

Characterization of the clones generated by the CRISPR/Cas9 method

We used a published DNA construct to target the *Smpd3* gene in MLOA5 cells. The multi-cistronic construct codes for a full guide RNA and Cas9 protein with a nuclear localization signal and carries a puromycin resistant cassette for selecting the stably transfected clones. Two BbSI sites allow easy cloning of a variable sequence for targeting any gene. The cloned targeting sequence will be expressed as a CRISPR RNA in unison with the constant tracrRNA to recruit the Cas9 protein (Fig.3).

We planned to disrupt the open reading frame (ORF) of *Smpd3* gene using the CRISPR/Cas9 approach. We expected to introduce double-stranded break within the (ORF) which will result in random insertions or deletions of nucleotide (indels), thus changing the reading frame. We used an online software resource to design the Smpd3 CRISPR RNA (E-crisp.com web and strider software to confirm) which selects the sequence with the least possibility of off targeting another sequence in the genome[78]. The suitability of the selected guide RNA was demonstrated by the high number of targeted clones carrying indels at the desired location of the *Smpd3* gene.

To know about the type of DNA modifications in our clones we first performed PCR and then Sanger sequencing of the amplified DNAs. Through this approach although we could identify the clones with indels, it appeared that most of the clones carried a wild type allele and a mutated allele. However, this method of sequence analyses was complicated as there were two peaks for each nucleotide position contributed by one wild type and one mutated or two

mutated alleles. Therefore, we designed a second strategy to first subclone the mixed PCR products and then sequence the plasmid DNA isolated from each individual clone. This way we were able to separate the PCR products generated from two different alleles.

Following the second strategy we first sequenced 3 subclones. If we detected a wild type sequence, this clone was not used. If no wild type sequence was detected, then another 3 subclones were sequenced. If again no wild type *Smpd3* sequence was detected, another 3 subclones were sent for sequencing (Table1). If altogether no wild type sequence was detected even after 9 sequencing attempts, and two different mutant clones were found, we considered the clone as a *Smpd3* 'knockout' clone (Fig.13)

Future use of the developed MLO-A5 models and their comparison with respective WT controls

The cultured MLOA5 cells treated with GW4869 showed reduced mineral deposition and showed a different pattern of mineral deposition presumably along the collagen network. In the second approach of the CRISPR/Cas9 knock out for *Smpd3* also similar reduction of mineral deposition was seen. Both these models can be used for the following future experiments:

For certain degree of relevance in cell culture models to the mineralization process as occurs physiologically *in vivo*, it is possible that the mineral crystals formed *in vitro* be of a true phase, shape, size, orientation, location, and crystallinity. So, systematic characterization of the minerals formed in these cultures, and mechanisms of extracellular matrix mineralization is needing a thorough comprehensive, multi-technique characterization of the morphology, composition, and ultrastructure of cell culture biomineral to determine their mineral phase. Advanced methods like X-ray diffraction (XRD), energy dispersive x-ray spectroscopy, Fourier transform infrared spectroscopy, scanning and transmission electron microscopy are

efficient to provide an insight into comparative study of mineral formed in *in vitro model* and wild type (WT) culture can be determined. Here, XRD through its electron diffraction patterns would allow to detect nano crystallinity of hydroxyapatites formed in the MLO-A5 models, which might differ from WT with higher crystalline nature of minerals. The energy dispersive x-ray spectroscopy is expected to confirm the culture mineral which consists of calcium and phosphates, including trace amounts of other minerals. Fourier transform infrared spectroscopy may also measure the amounts of apatitic carbonate and phosphate. The above methods would aid to specifically distinguish mineral phases of MLO-A5 models from WT culture. While ultrastructural analysis with scanning and transmission electron microscopy may show a difference in cultures which will have a dense and assembled collagenous matrix where with size and shape of collagen-associated mineralization which form mineral aggregates in WT culture vs. our MLO-A5 models. Additionally, a confocal imaging and the three-dimensional reconstructions should reveal if biology has undergone a change in MLO-A5 models in terms of cells that should generally exhibit dendritic processes and become embedded within the mineral in an osteocyte-like manner. By this, we can characterize the mineral phase deposited on monolayer cultures of MLO-A5 models as well as WT cells and would let us determine the structural and compositional properties of their minerals, which can be compared to that of *in-vivo* models of bone mineralization.

Matrix Vesicles (MVs) isolation, number quantification and characterization from MLO-A5 models as well as WT cells.

MVs can be isolated from MLO-A5 cell cultures with joint use of ultracentrifugation and gradient centrifugation and alternatively, by differential centrifugation of trypsin digests of the cell layer, which will be used for separation of the cells from the digest supernatant and a

further longer spin down for the fraction of MVs pellet by fractionation on a sucrose gradient[36, 104,105]. Another effective method of isolation could be immunoprecipitation[105]. Extraction of MVs may be done from mineralizing cells in culture after two days of treatment to 10 days of treatment, (i.e., time interval could be 2, 4, 6, 8 and 10 days). To visualize MVs nanoparticle tracking analysis and atomic force microscopy can be used to analyze matrix vesicle size, shape, ultrastructure, and concentration within the culture medium of constructs[106,107]. It is expected that the numbers of MVs might be lower in knockout group than in WT group of cells, similarly, should be the case with its mineral contents and levels of SMPD3.

Limitations of the study and strategy to address them

Out of 9 transfected single cell cultured clones, in order to generate a knockout clone, many attempts were made. First, we screened clone 1 using cloning and subcloning strategy to detect a WT allele. Eight subclones were sequenced and analyzed, then we noticed the presence of 3 alleles which said the possibility that this could be a mixed clone. In this case, even though the vector is expressed constitutively in the cells, the clones might have lost it at a certain stage and even mixed clones may give rise to rescued gene expression despite the antibiotic selection treatment. Therefore, we had to eliminate clone 1 from further experiments.

The second time we detected a heterozygote clone (clone 1.1) since we recorded the presence of one WT allele and another altered allele; therefore, this clone was too excluded. The third time, we subcloned a single cell ‘clone 2’ for 6 times and we did not come across any presence of WT allele. This clone 2 was ascertained as a complete knockout model clone since both alleles were altered as such mutations were considered homozygous.

The screening method of sub cloning needed several repetitions and so needed a significant amount of time in which technical challenges were also faced, re-established protocol and

resolved. One strategy that can be used to tackle the scenario and save time is by doing a regular PCR with forward and reverse primers targeting the region of mutation with an amplicon size of less than 200 bps. In this way, all the potential clones can be analyzed at the same time. However, mostly we observed during the screening of potential clones that there were a high number of single alleles being targeted, resulting in heterozygous clones. Subcloning method used to segregate the alleles in knockout model has been prolonging due to the low copy numbers of plasmid which used to result in low yield of bacterial culture and often concentration of mini-prep samples were low causing subsequent repeats for every clone.

Since a simultaneous effort was taken in generating a knockout clone and characterizing these clones via in-vitro mineralization assays, analyzing their gene expression, checking for mineral properties; it was time consuming that we now lacked duration for the proposed experiments to establish method for isolation of Matrix vesicles and their characterization from the MLO-A5 models developed in our study. At the same time, our models are based on a single cell-line MLO-A5, a pre-osteocytic cell type that gets differentiated into osteocytes after several treatments of differentiation, due to which they may show low *Smpd3* gene expression levels which may not give comparable data for knockout model vs. WT control. Alternatively, MC3T3.E1, a pre-osteoblastic cell line would be useful to see their mineralization properties and SMPD3 expression.

CHAPTER 6: CONCLUSION

In this study, we have observed that the poor mineralization is due to the reduced and inactive expression of SMPD3 enzyme in the pre-osteocytic MLO-A5 cell models. In a pharmacologic approach, we established an MLO-A5 model with decreased mineralization by chemical inhibition of SMPD3. In the CRISPR CAS-9 gene target-based method, we successfully generated a *Smpd3* gene knockout model which resulted in lack of normal mineralization in MLO-A5 cells cultured. We also characterized the knockout model by gene expression analysis before the differentiation of MLO-A5 cells and recorded the difference in expression levels which were significantly lower in knockout group than the WT group. SEM analysis also showed that nature of mineral phases among the MLO-A5 models and controls matched. It was also noted that the content of Calcium-Phosphates was found to be more in WT samples than the knockout group. Therefore, we conclude that the above characterized MLO-A5 models can be reliably used for future experiments on MVs isolation and characterization. This may possibly bridge the gap in knowledge about the secretion of MVs from bone cells and their role in the pathway of bone biomineralization.

CHAPTER 7: REFERENCES

1. Cohen, P. A., Strauss, J. V., Rooney, A. D., Sharma, M., & Tosca, N. (2017). Controlled hydroxyapatite biomineralization in an~ 810-million-year-old unicellular eukaryote. *Science Advances*, *3*(6), e1700095.

2. Hazen, R. M., Papineau, D., Bleeker, W., Downs, R. T., Ferry, J. M., McCoy, T. J., ... & Yang, H. (2008). Mineral evolution. *American Mineralogist*, *93*(11-12), 1693-1720.

3. Knoll, A. H. (2003). Biomineralization and evolutionary history. *Reviews in mineralogy and geochemistry*, *54*(1), 329-356.

4. Weiner, S., & Dove, P. M. (2003). An overview of biomineralization processes and the problem of the vital effect. *Reviews in mineralogy and geochemistry*, *54*(1), 1-29.

5. Allison, C. W., & Hilgert, J. W. (1986). Scale microfossils from the Early Cambrian of northwest Canada. *Journal of Paleontology*, *60*(5), 973-1015.

6. Thingstad, T. F., Krom, M. D., Mantoura, R. F. C., Flaten, G. F., Groom, S., Herut, B., ... & Zohary, T. (2005). Nature of phosphorus limitation in the ultraoligotrophic eastern Mediterranean. *Science*, *309*(5737), 1068-1071.

7. Macdonald, F. A., Cohen, P. A., Dudás, F. Ő., & Schrag, D. P. (2010). Early Neoproterozoic scale microfossils in the lower Tindir Group of Alaska and the Yukon Territory. *Geology*, *38*(2), 143-146.

8. Wagner DO, Aspenberg P. 2011. Where did bone come from? Acta Orthop 82: 393–398.

9. Murshed, M. (2018). Mechanism of bone mineralization. *Cold Spring Harbor perspectives in medicine*, *8*(12), a031229.

10. Zhang, G., & Cohn, M. J. (2006). Hagfish and lancelet fibrillar collagens reveal that type II collagen-based cartilage evolved in stem vertebrates. *Proceedings of the National Academy of Sciences*, *103*(45), 16829-16833.

11. Tarazona, O. A., Slota, L. A., Lopez, D. H., Zhang, G., & Cohn, M. J. (2016). The genetic program for cartilage development has deep homology within Bilateria. *Nature*, *533*(7601), 86-89.

12. Donoghue, Philip CJ, and Ivan J. Sansom. "Origin and early evolution of vertebrate skeletonization." *Microscopy research and technique* 59.5 (2002): 352-372.

13. Maisey, J. G., Denton, J. S., Burrow, C., & Pradel, A. (2021). Architectural and ultrastructural features of tessellated calcified cartilage in modern and extinct chondrichthyan fishes. *Journal of Fish Biology*, *98*(4), 919-941.

14. Ryll, B., Sanchez, S., Haitina, T., Tafforeau, P., & Ahlberg, P. E. (2014). The genome of Callorhinchus and the fossil record: a new perspective on SCPP gene evolution in gnathostomes. *Evolution & Development*, *16*(3), 123.

15. Enault, S., Muñoz, D. N., Silva, W. T., Borday-Birraux, V., Bonade, M., Oulion, S., ... & Debiais-Thibaud, M. (2015). Molecular footprinting of skeletal tissues in the catshark Scyliorhinus canicula and the clawed frog Xenopus tropicalis identifies conserved and derived features of vertebrate calcification. *Frontiers in genetics*, *6*, 283.

16. Debiais-Thibaud, M., Simion, P., Ventéo, S., Muñoz, D., Marcellini, S., Mazan, S., & Haitina, T. (2019). Skeletal mineralization in association with type X collagen expression is an ancestral feature for jawed vertebrates. *Molecular biology and evolution*, *36*(10), 2265-2276.

17. Leurs, N., Martinand-Mari, C., Ventéo, S., Haitina, T., & Debiais-Thibaud, M. (2021). Evolution of matrix gla and bone gla protein genes in jawed vertebrates. *Frontiers in genetics*, 245.

18. Eames, B. F., Allen, N., Young, J., Kaplan, A., Helms, J. A., & Schneider, R. A. (2007). Skeletogenesis in the swell shark Cephaloscyllium ventriosum. *Journal of anatomy*, *210*(5), 542-554.

19. Seidel, R., Blumer, M., Pechriggl, E. J., Lyons, K., Hall, B. K., Fratzl, P., ... & Dean, M. N. (2017). Calcified cartilage or bone? Collagens in the tessellated endoskeletons of cartilaginous fish (sharks and rays). *Journal of structural biology*, *200*(1), 54-71.

20. Atake, O. J., Cooper, D. M., & Eames, B. F. (2019). Bone-like features in skate suggest a novel elasmobranch synapomorphy and deep homology of trabecular mineralization patterns. *Acta biomaterialia*, *84*, 424-436.

21. Meredith Smith, M., Underwood, C., Goral, T., Healy, C., & Johanson, Z. (2019). Growth and mineralogy in dental plates of the holocephalan Harriotta raleighana (Chondrichthyes): novel dentine and conserved patterning combine to create a unique chondrichthyan dentition. *Zoological letters*, *5*(1), 1-30.

22. Chaumel, J., Schotte, M., Bizzarro, J. J., Zaslansky, P., Fratzl, P., Baum, D., & Dean, M. N. (2020). Co-aligned chondrocytes: zonal morphological variation and structured arrangement of cell lacunae in tessellated cartilage. *Bone*, *134*, 115264.

23. Pears, J. B., Johanson, Z., Trinajstic, K., Dean, M. N., & Boisvert, C. A. (2020). Mineralization of the callorhinchus vertebral column (Holocephali; Chondrichthyes). *Frontiers in Genetics*, *11*, 571694.

24. Witten, P. E., & Huysseune, A. (2009). A comparative view on mechanisms and functions of skeletal remodelling in teleost fish, with special emphasis on osteoclasts and their function. *Biological Reviews*, *84*(2), 315-346.

25. Hall, B. K., & Witten, P. E. (2018). Plasticity and variation of skeletal cells and tissues and the evolutionary development of actinopterygian fishes. *Evolution and development of fishes*, 126-143.

26. Witten, P. E., Huysseune, A., & Hall, B. K. (2010). A practical approach for the identification of the many cartilaginous tissues in teleost fish. *Journal of Applied Ichthyology*, *26*(2), 257-262.

27. Giachelli C. M. (1999). Ectopic calcification: gathering hard facts about soft tissue mineralization. *The American journal of pathology*, *154*(3), 671–675. https://doi.org/10.1016/S0002-9440(10)65313-8

28. Golub E. E. (2009). Role of matrix vesicles in biomineralization. Biochimica et biophysica acta, 1790(12), 1592–1598. https://doi.org/10.1016/j.bbagen.2009.09.006

29. McKee, M. D., Hoac, B., Addison, W. N., Barros, N. M., Millán, J. L., & Chaussain, C. (2013). Extracellular matrix mineralization in periodontal tissues: Noncollagenous matrix proteins, enzymes, and relationship to hypophosphatasia and X-linked hypophosphatemia. *Periodontology 2000*, *63*(1), 102–122. https://doi.org/10.1111/prd.12029

30. A.S. Cole, J.E. Eastoe,Chapter 28 - Biological mineral, Editor(s): A.S. Cole, J.E. Eastoe, Biochemistry and Oral Biology (Second Edition), Butterworth-Heinemann, 1988, Pages 425-434, ISBN 9780723617518, https://doi.org/10.1016/B978-0-7236-1751-8.50035-1

31. Yu, T., & Klein, O. D. (2020). Molecular and cellular mechanisms of tooth development, homeostasis and repair. *Development (Cambridge, England)*, *147*(2), dev184754. https://doi.org/10.1242/dev.184754

32. Ikeda, Etsuko & Tsuji, Takashi. (2008). Growing bioengineered teeth from single cells: Potential for dental regenerative medicine. Expert opinion on biological therapy. 8. 735-44. 10.1517/14712598.8.6.735.

33. Lacruz, R. S., Habelitz, S., Wright, J. T., & Paine, M. L. (2017). DENTAL ENAMEL FORMATION AND IMPLICATIONS FOR ORAL HEALTH AND DISEASE. *Physiological reviews*, *97*(3), 939–993. https://doi.org/10.1152/physrev.00030.2016

34. Boskey, A. L., & Roy, R. (2008). Cell culture systems for studies of bone and tooth mineralization. *Chemical reviews*, *108*(11), 4716–4733. https://doi.org/10.1021/cr0782473.

35. Boyde, A. (1989). Enamel. In *Teeth* (pp. 309-473). Springer, Berlin, Heidelberg. https://www-sciencedirect-com.proxy3.library.mcgill.ca/science/article/pii/S0097052234904469

36. Hasegawa T. (2018). Ultrastructure and biological function of matrix vesicles in bone mineralization. Histochemistry and cell biology, 149(4), 289–304. https://doi.org/10.1007/s00418-018-1646-0

37. Yamamoto, T., Hasegawa, T., Yamamoto, T., Hongo, H., & Amizuka, N. (2016). Histology of human cementum: Its structure, function, and development. *Japanese dental science review*, *52*(3), 63-74.

38. Haraguchi, R., Kitazawa, R., Imai, Y., & Kitazawa, S. (2018). Growth plate-derived hedgehog-signal-responsive cells provide skeletal tissue components in growing bone. *Histochemistry and Cell Biology*, *149*(4), 365-373.

39. Yagami, K., Suh, J. Y., Enomoto-Iwamoto, M., Koyama, E., Abrams, W. R., Shapiro, I. M.,.. & Iwamoto, M. (1999). Matrix GLA protein is a developmental regulator of chondrocyte mineralization and, when constitutively expressed, blocks endochondral and intramembranous ossification in the limb. *The Journal of cell biology*, *147*(5), 1097-1108.

40. Hallett, S. A., Ono, W., & Ono, N. (2019). Growth Plate Chondrocytes: Skeletal Development, Growth and Beyond. *International journal of molecular sciences*, *20*(23), 6009. https://doi.org/10.3390/ijms20236009

41. Kronenberg, H. M. (2003). Developmental regulation of the growth plate. *Nature*, *423*(6937), 332-336.

42. *Cartilage*. Physiopedia. (n.d.). Retrieved September 30, 2022, from https://www.physiopedia.com/Cartilage

43. Kojima, T., Hasegawa, T., De Freitas, P. H. L., Yamamoto, T., Sasaki, M., Horiuchi, K., ... & Amizuka, N. (2013). Histochemical aspects of the vascular invasion at the erosion zone of the epiphyseal cartilage in MMP-9-deficient mice. *Biomedical Research*, *34*(3), 119-128.

44. Tsang, K. Y., Chan, D., & Cheah, K. S. (2015). Fate of growth plate hypertrophic chondrocytes: death or lineage extension. *Development, growth & differentiation*, *57*(2), 179-192.

45. Wallis, Gillian A. "Bone growth: coordinating chondrocyte differentiation." *Current Biology* 6.12 (1996): 1577-1580.

46. Gerber, H. P., Vu, T. H., Ryan, A. M., Kowalski, J., Werb, Z., & Ferrara, N. (1999). VEGF couples hypertrophic cartilage remodeling, ossification and angiogenesis during endochondral bone formation. *Nature medicine*, *5*(6), 623-628.

47. Mohamed, A. M. (2008). An overview of bone cells and their regulating factors of differentiation. *The Malaysian journal of medical sciences: MJMS*, *15*(1), 4.

48. Wu, X., Dai, H., Yu, S., Zhao, Y., Long, Y., Li, W., & Tu, J. (2021). Citrate regulates extracellular matrix mineralization during osteoblast differentiation in vitro. *Journal of Inorganic Biochemistry*, *214*, 111269.

49. Arkady Rutkovskiy A., Stensløkken K., Vaage I.J. Osteoblast differentiation at a glance. *Med. Sci. Monit. Basic Res.* 2016;22:95–106. doi: 10.12659/MSMBR.901142.

50. DiGirolamo C.M., Stokes D., Colter D., Phinney D.G., Class R., Prockop D.J. Propagation and senescence of human marrow stromal cells in culture: A simple colony-forming assay identifies samples with the greatest potential to propagate and differentiate. *Br. J. Haematol.* 1999;107:275–281. doi: 10.1046/j.1365-2141.1999.01715.x.

51. Friedenstein A.J., Chailakhyan R.K., Gerasimov U.V. Bone marrow osteogenic stem cells: In vitro cultivation and transplantation in diffusion chambers. *Cell Tissue Kinet.* 1987;20:263–272. doi: 10.1111/j.1365-2184.1987.tb01309.x.

52. Ducy P., Schinke T., Karsenty G. The Osteoblast: A Sophisticated Fibroblast under Central Surveillance. *Science.* 2000;289:1501–1504. doi: 10.1126/science.289.5484.1501

53. Ducy P., Desbois C., Boyce B., Pinero G., Story B., Dunstan C., Smith E., Bonadio J., Goldstein S., Gundberg C., et al. Increased bone formation in osteocalcin-deficient mice. *Nature.* 1996;382:448–452. doi: 10.1038/382448a0.

54. Denu R.A., Nemcek S., Bloom D.D., Goodrich A.D., Kim J., Mosher D.F., Hematti P. Fibroblasts and Mesenchymal Stromal/Stem Cells Are Phenotypically Indistinguishable. *Acta Haematol.* 2016;136:85–97. doi: 10.1159/000445096

55. Chung C.H., Golub E.E., Forbes E., Tokuoka T., Shapiro I.M. Mechanism of action of β-glycerophosphate on bone cell mineralization. *Calcif. Tissue Int.* 1992;51:305–311. doi: 10.1007/BF00334492.

56. Gregory C.A., Gunn W.G., Peister A., Prockop D.J. An Alizarin red-based assay of mineralization by adherent cells in culture: Comparison with cetylpyridinium chloride extraction. *Anal. Biochem.* 2004;329:77–84. doi: 10.1016/j.ab.2004.02.002.

57. Murshed, M., & McKee, M. D. (2010). Molecular determinants of extracellular matrix mineralization in bone and blood vessels. Current opinion in nephrology and hypertension, 19(4), 359–365. https://doi.org/10.1097/MNH.0b013e3283393a2b

58. Franz-Odendaal, T. A., Hall, B. K., & Witten, P. E. (2006). Buried alive: how osteoblasts become osteocytes. *Developmental dynamics: an official publication of the American Association of Anatomists*, *235*(1), 176-190.

59. Stewart, A. J., Roberts, S. J., Seawright, E., Davey, M. G., Fleming, R. H., & Farquharson, C. (2006). The presence of PHOSPHO1 in matrix vesicles and its developmental expression prior to skeletal mineralization. Bone, 39(5), 1000–1007. https://doi.org/10.1016/j.bone.2006.05.014

60. Roberts, S., Narisawa, S., Harmey, D., Millán, J. L., & Farquharson, C. (2007). Functional involvement of PHOSPHO1 in matrix vesicle-mediated skeletal mineralization. Journal of bone and mineral research: the official journal of the American Society for Bone and Mineral Research, 22(4), 617–627. https://doi.org/10.1359/jbmr.070108

61. MacRae, V. E., Davey, M. G., McTeir, L., Narisawa, S., Yadav, M. C., Millan, J. L., & Farquharson, C. (2010). Inhibition of PHOSPHO1 activity results in impaired skeletal mineralization during limb development of the chick. *Bone*, *46*(4), 1146-1155.

62. Aubin, I., Adams, C. P., Opsahl, S., Septier, D., Bishop, C. E., Auge, N., ... & Poirier, C. (2005). A deletion in the gene encoding sphingomyelin phosphodiesterase 3 (Smpd3) results in osteogenesis and dentinogenesis imperfecta in the mouse. *Nature genetics*, *37*(8), 803-805.

63. Yadav, M. C., Simao, A. M. S., Narisawa, S., Huesa, C., McKee, M. D., Farquharson, C., & Millán, J. L. (2011). Loss of skeletal mineralization by the simultaneous ablation of PHOSPHO1 and alkaline phosphatase function: a unified model of the mechanisms of initiation of skeletal calcification. *Journal of Bone and Mineral Research*, *26*(2), 286-297.

64. Stoffel W, Jenke B, Holz B, Binczek E, Günter RH, Knifka J, Koebke J, Niehoff A. 2007. Neutral sphingomyelinase (SMPD3) deficiency causes a novel form of chondrodysplasia

65. Stoffel, W., Jenke, B., Blöck, B., Zumbansen, M., & Koebke, J. (2005). Neutral sphingomyelinase 2 (smpd3) in the control of postnatal growth and development. *Proceedings of the National Academy of Sciences*, *102*(12), 4554-4559.

66. Menck, K., Sönmezer, C., Worst, T. S., Schulz, M., Dihazi, G. H., Streit, F., Erdmann, G., Kling, S., Boutros, M., Binder, C., & Gross, J. C. (2017). Neutral sphingomyelinases control extracellular vesicles budding from the plasma membrane. Journal of extracellular vesicles, 6(1), 1378056. https://doi.org/10.1080/20013078.2017.1378056

67. Li, J., Manickam, G., Ray, S., Oh, C. D., Yasuda, H., Moffatt, P., & Murshed, M. (2016). Smpd3 Expression in both Chondrocytes and Osteoblasts Is Required for Normal Endochondral Bone Development. Molecular and cellular biology, 36(17), 2282–2299. https://doi.org/10.1128/MCB.01077-15

68. Khavandgar, Z., & Murshed, M. (2015). Sphingolipid metabolism and its role in the skeletal tissues. Cellular and molecular life sciences: CMLS, 72(5), 959–969. https://doi.org/10.1007/s00018-014-1778-x

69. Holland, W. L., Brozinick, J. T., Wang, L. P., Hawkins, E. D., Sargent, K. M., Liu, Y., ... & Summers, S. A. (2007). Inhibition of ceramide synthesis ameliorates glucocorticoid-, saturated-fat-, and obesity-induced insulin resistance. *Cell metabolism*, *5*(3), 167-179.

70. Stewart, A. J., Leong, D. T. K., & Farquharson, C. (2018). PLA2 and ENPP6 may act in concert to generate phosphocholine from the matrix vesicle membrane during skeletal mineralization. FASEB Journal, 32(1), 20-25. https://doi.org/10.1096/fj.201700521r

71. Berio, F., Broyon, M., Enault, S., Pirot, N., López-Romero, F. A., & Debiais-Thibaud, M. (2021). Diversity and evolution of mineralized skeletal tissues in chondrichthyans. *Frontiers in Ecology and Evolution*, *9*, 660767.

72. del Mar Arriero, M., Ramis, J. M., Perelló, J., & Monjo, M. (2012). Differential response of MC3T3-E1 and human mesenchymal stem cells to inositol hexakisphosphate. *Cellular Physiology and Biochemistry*, *30*(4), 974-986.

73. Sudo, H., Kodama, H. A., Amagai, Y., Yamamoto, S., & Kasai, S. (1983). In vitro differentiation and calcification in a new clonal osteogenic cell line derived from newborn mouse calvaria. *The Journal of cell biology*, *96*(1), 191-198.

74. Addison, W. N., Nelea, V., Chicatun, F., Chien, Y. C., Tran-Khanh, N., Buschmann, M. D., ... & McKee, M. D. (2015). Extracellular matrix mineralization in murine MC3T3-E1 osteoblast cultures: an ultrastructural, compositional, and comparative analysis with mouse bone. *Bone*, *71*, 244-256.

75. Iordachescu, A., Hulley, P., & Grover, L. M. (2018). A novel method for the collection of nanoscopic vesicles from an organotypic culture model. RSC advances, 8(14), 7622–7632. https://doi.org/10.1039/c7ra12511a

76. Cui, L., Houston, D. A., Farquharson, C., & MacRae, V. E. (2016). Characterization of matrix vesicles in skeletal and soft tissue mineralization. Bone, 87, 147–158. https://doi.org/10.1016/j.bone.2016.04.007

77. Hynes, A. P., Villion, M., & Moineau, S. (2014). Adaptation in bacterial CRISPR-Cas immunity can be driven by defective phages. *Nature Communications*, *5*(1), 1-6.

78. Zhang, Y., & Showalter, A. M. (2020). CRISPR/Cas9 genome editing technology: a valuable tool for understanding plant cell wall biosynthesis and function. *Frontiers in Plant Science*, *11*, 589517.

79. Jinek, M., Chylinski, K., Fonfara, I., Hauer, M., Doudna, J. A., & Charpentier, E. (2012). A programmable dual-RNA–guided DNA endonuclease in adaptive bacterial immunity. *science*, *337*(6096), 816-821.

80. Wiedenheft, B., Sternberg, S. H., & Doudna, J. A. (2012). RNA-guided genetic silencing systems in bacteria and archaea. *Nature*, *482*(7385), 331-338.

81. Synthego.com. 2022. *Synthego | Full Stack Genome Engineering*. [online] Available at: <https://www.synthego.com/blog/rnai-vs-crispr-guide> [Accessed 1 October 2022].

82. Gao, Y., & Zhao, Y. (2014). Self-processing of ribozyme-flanked RNAs into guide RNAs in vitro and in vivo for CRISPR-mediated genome editing. *Journal of integrative plant biology*, *56*(4), 343-349.

83. Jiang, F., & Doudna, J. A. (2017). CRISPR-Cas9 structures and mechanisms. *Annu Rev Biophys*, *46*(1), 505-529.

84. Jiang, W., Bikard, D., Cox, D., Zhang, F., & Marraffini, L. A. (2013). RNA-guided editing of bacterial genomes using CRISPR-Cas systems. *Nature biotechnology*, *31*(3), 233-239.

85. Moreno-Mateos, M. A., Vejnar, C. E., Beaudoin, J. D., Fernandez, J. P., Mis, E. K., Khokha, M. K., & Giraldez, A. J. (2015). CRISPRscan: designing highly efficient sgRNAs for CRISPR-Cas9 targeting in vivo. *Nature methods*, *12*(10), 982-988.

86. Samarut, É., Lissouba, A., & Drapeau, P. (2016). A simplified method for identifying early CRISPR-induced indels in zebrafish embryos using High Resolution Melting analysis. *BMC genomics*, *17*(1), 1-6.

87. Liu, X., Homma, A., Sayadi, J., Yang, S., Ohashi, J., & Takumi, T. (2016). Sequence features associated with the cleavage efficiency of CRISPR/Cas9 system. *Scientific reports*, *6*(1), 1-9.

88. Gagnon, J. A., Valen, E., Thyme, S. B., Huang, P., Ahkmetova, L., Pauli, A., ... & Schier, A. F. (2014). Efficient mutagenesis by Cas9 protein-mediated oligonucleotide insertion and large-scale assessment of single-guide RNAs. *PloS one*, *9*(5), e98186.

89. Ma, X., & Liu, Y. G. (2016). CRISPR/Cas9-based multiplex genome editing in monocot and dicot plants. *Current protocols in molecular biology*, *115*(1), 31-6.

90. Ma, X., Zhang, Q., Zhu, Q., Liu, W., Chen, Y., Qiu, R., ... & Liu, Y. G. (2015). A robust CRISPR/Cas9 system for convenient, high-efficiency multiplex genome editing in monocot and dicot plants. *Molecular plant*, *8*(8), 1274-1284.

91. Liang, Y., Basu, D., Pattathil, S., Xu, W. L., Venetos, A., Martin, S. L., ... & Showalter, A. M. (2013). Biochemical and physiological characterization of fut4 and fut6 mutants defective in arabinogalactan-protein fucosylation in Arabidopsis. *Journal of experimental botany*, *64*(18), 5537-5551.

92. Kato, Y., Boskey, A., Spevak, L., Dallas, M., Hori, M., & Bonewald, L. F. (2001). Establishment of an osteoid preosteocyte-like cell MLO-A5 that spontaneously mineralizes in culture. *Journal of Bone and Mineral Research*, *16*(9), 1622-1633.

93. Blair, H. C., Larrouture, Q. C., Li, Y., Lin, H., Beer-Stoltz, D., Liu, L., ... & Nelson, D. J. (2017). Osteoblast differentiation and bone matrix formation in vivo and in vitro. *Tissue Engineering Part B: Reviews*, *23*(3), 268-280.

94. Orriss, I. R., Arnett, T. R., & Russell, R. G. G. (2016). Pyrophosphate: a key inhibitor of mineralisation. *Current opinion in pharmacology*, *28*, 57-68.

95. Gjorgjieva, T., Xie, X., Commins, P., Pasricha, R., Mahmood, S. R., Gunsalus, K. C., ... & Percipalle, P. (2020). Loss of β-actin leads to accelerated mineralization and dysregulation of osteoblast-differentiation genes during osteogenic reprogramming. *Advanced Science*, *7*(23), 2002261

96. Rosser, J., & Bonewald, L. F. (2012). Studying osteocyte function using the cell lines MLO-Y4 and MLO-A5. In *Bone research protocols* (pp. 67-81). Humana Press, Totowa, NJ.

97. Donzelli, E., Salvade, A., Mimo, P., Viganò, M., Morrone, M., Papagna, R., ... & Tredici, G. (2007). Mesenchymal stem cells cultured on a collagen scaffold: In vitro osteogenic differentiation. *Archives of oral biology*, *52*(1), 64-73.

98. Schlesinger, P. H., Blair, H. C., Beer Stolz, D., Riazanski, V., Ray, E. C., Tourkova, I. L., & Nelson, D. J. (2020). Cellular and extracellular matrix of bone, with principles of synthesis and dependency of mineral deposition on cell membrane transport. *American Journal of Physiology-Cell Physiology*, *318*(1), C111-C124.

99. Schroeder, T. M., Jensen, E. D., & Westendorf, J. J. (2005). Runx2: a master organizer of gene transcription in developing and maturing osteoblasts. *Birth Defects Research Part C: Embryo Today: Reviews*, *75*(3), 213-225.

100. Essandoh, K., Yang, L., Wang, X., Huang, W., Qin, D., Hao, J., Wang, Y., Zingarelli, B., Peng, T., & Fan, G. C. (2015). Blockade of exosome generation with GW4869 dampens the sepsis-induced inflammation and cardiac dysfunction. *Biochimica et biophysica acta*, *1852*(11), 2362–2371. https://doi.org/10.1016/j.bbadis.2015.08.010

101. Kulshreshtha, A., Ahmad, T., Agrawal, A., & Ghosh, B. (2013). Proinflammatory role of epithelial cell–derived exosomes in allergic airway inflammation. *Journal of allergy and clinical immunology*, *131*(4), 1194-1203

102. Kosaka, N., Iguchi, H., Yoshioka, Y., Takeshita, F., Matsuki, Y., & Ochiya, T. (2010). Secretory mechanisms and intercellular transfer of microRNAs in living cells. *Journal of Biological Chemistry*, *285*(23), 17442-174

103. Li, J., Liu, K., Liu, Y., Xu, Y., Zhang, F., Yang, H., ... & Yuan, Z. (2013). Exosomes mediate the cell-to-cell transmission of IFN-α-induced antiviral activity. *Nature immunology*, *14*(8), 793-803.

104. Murshed, M., Harmey, D., Millán, J. L., McKee, M. D., & Karsenty, G. (2005). Unique co-expression in osteoblasts of broadly expressed genes accounts for the spatial restriction of ECM mineralization to bone. *Genes & development*, *19*(9), 1093-1104.

105. Balcerzak, M., Radisson, J., Azzar, G., Farlay, D., Boivin, G., Pikula, S., & Buchet, R. (2007). A comparative analysis of strategies for isolation of matrix vesicles. Analytical biochemistry, 361(2), 176–182. https://doi.org/10.1016/j.ab.2006.10.001

106. Boskey, A. L. (2001). Bone Biomechanics.

107. Boskey, A., & Pleshko Camacho, N. (2007). FT-IR imaging of native and tissue-engineered bone and cartilage. *Biomaterials*, *28*(15), 2465–2478. https://doi.org/10.1016/j.biomaterials.2006.11.043

108. Jaiswal, N., Haynesworth, S. E., Caplan, A. I., & Bruder, S. P. (1997). Osteogenic differentiation of purified, culture-expanded human mesenchymal stem cells in vitro. *Journal of cellular biochemistry*, *64*(2), 295-312.

109. Bonjour, J. P. (2011). Calcium and phosphate: a duet of ions playing for bone health. *Journal of the American College of Nutrition*, *30*(sup5), 438S-448S.

110. Anderson, H. C., Hsu, H. H., Morris, D. C., Fedde, K. N., & Whyte, M. P. (1997). Matrix vesicles in osteomalacic hypophosphatasia bone contain apatite-like mineral crystals. The American journal of pathology, 151(6), 1555–1561.

111. Buchet, R., Pikula, S., Magne, D., & Mebarek, S. (2013). Isolation and characteristics of matrix vesicles. In *Phosphatase Modulators* (pp. 115-124). Humana Press, Totowa, NJ.

112. T. Hasegawa, H. Hongo, T. Yamamoto, M. Abe, H. Yoshino, M. Haraguchi-Kitakamae, et al. Int J Mol Sci 2022 Vol. 23 Issue 17, Accession Number: 36077336 PMCID: PMC9456179 DOI: 10.3390/ijms23179941; https://www.ncbi.nlm.nih.gov/pubmed/36077336

113. Berio, F., Broyon, M., Enault, S., Pirot, N., López-Romero, F. A., & Debiais-Thibaud, M. (2021). Diversity and evolution of mineralized skeletal tissues in chondrichthyans. *Frontiers in Ecology and Evolution*, *9*, 660767.

114. Sheldon H, Robinson RA. 1957. Electron microscope studies of crystal-collagen relationships in bone. IV: The occurrence of crystals within collagen fibrils. J Biophys Biochem Cytol 3: 1011–1016.

115. Tian, E., Watanabe, F., Martin, B., & Zangari, M. (2020). Innate biomineralization. *International journal of molecular sciences*, *21*(14), 4820.

116. Boskey, A. L., Moore, D. J., Amling, M., Canalis, E., & Delany, A. M. (2003). Infrared analysis of the mineral and matrix in bones of osteonectin-null mice and their wildtype controls. *Journal of Bone and Mineral Research*, *18*(6), 1005-1011.

117. Boskey, A. L., Boyan, B. D., & Schwartz, Z. (1997). Matrix vesicles promote mineralization in a gelatin gel. Calcified tissue international, 60(3), 309–315. https://doi.org/10.1007/s002239900234

118. Manickam, G., Moffatt, P., & Murshed, M. (2019). Role of SMPD3 during Bone Fracture Healing and Regulation of Its Expression. Molecular and cellular biology, 39(4), e00370-18. https://doi.org/10.1128/MCB.00370-18

119. Fibbe, W. E. (2002). Mesenchymal stem cells. A potential source for skeletal repair. *Annals of the rheumatic diseases*, *61*(suppl 2), ii29-ii31.

120. Mebarek S, Abousalham A, Magne D, Do le D, Bandorowicz- Pikula J, Pikula S, Buchet R. 2013. Phospholipases of mineralization competent cells and matrix vesicles: Roles in physiological and pathological mineralizations. Int J Mol Sci 14: 5036–5129.

121. Thouverey, Cyril & Balcerzak, Marcin & Strzelecka-Kiliszek, Agnieszka & Pikula, Slawomir & Buchet, René. (2008). Origin of matrix vesicles in mineralization competent osteoblast-like saos-2 cells. Bone. 42. https://doi.org/10.1016/j.bone.2007.12.045

122. PSpCas9(BB)-2A-Puro (PX459) V2.0 (Plasmid #62988). (n.d.). Retrieved November 14, 2020, from https://www.addgene.org/62988/

123. Gilbert SF. Developmental Biology. 6th edition. Sunderland (MA): Sinauer Associates; 2000. Osteogenesis: The Development of Bones. Available from: https://www.ncbi.nlm.nih.gov/books/NBK10056/

124. Stoffel, W., Hammels, I., Jenke, B., Schmidt-Soltau, I., & Niehoff, A. (2019). Neutral Sphingomyelinase 2 (SMPD3) Deficiency in Mice Causes Chondrodysplasia with Unimpaired Skeletal Mineralization. The American journal of pathology, 189(9), 1831–1845. https://doi.org/10.1016/j.ajpath.2019.05.008

125. Kirsch, T., Nah, H. D., Shapiro, I. M., & Pacifici, M. (1997). Regulated production of mineralization-competent matrix vesicles in hypertrophic chondrocytes. The Journal of cell biology, 137(5), 1149–1160. https://doi.org/10.1083/jcb.137.5.1149

126. Nannuru, K. C., & Singh, R. K. (2010). Tumor-stromal interactions in bone metastasis. *Current osteoporosis reports*, *8*(2), 105-113.